Journal of Hydrometeorology

Performance evaluation of a new dual-polarization microphysical algorithm based on long-term X-band radar and disdrometer observations

--Manuscript Draft--

Manuscript Number:	JHM-D-12-057
Full Title:	Performance evaluation of a new dual-polarization microphysical algorithm based on long-term X-band radar and disdrometer observations
Article Type:	Article
Corresponding Author:	Marios N. Anagnostou, Ph.D Sapienza University of Rome Rome, ITALY
Corresponding Author's Institution:	Sapienza University of Rome
First Author:	Marios N. Anagnostou, Ph.D
Order of Authors:	Marios N. Anagnostou, Ph.D
	John Kalogiros, Ph.D
	Frank Silvio Marzano, Ph.D
	Emmanouil N. Anagnostou, Ph.D
	Mario Montopoli, Ph.D
	Erricio Piccioti, Ph.D
Abstract:	Accurate estimation of precipitation at high spatial and temporal resolution of weather radars is an open problem in hydrometeorological applications. The use of dual-polarization gives the advantage of multiparameter measurements using orthogonal polarization states. These measurements carry significant information, useful for estimating rain-path signal attenuation, raindrop size distribution (DSD) and rainfall rate. This study evaluates a new Self-Consistent with Optimal Parameterization attenuation correction and rain Microphysics Estimation algorithm (named SCOP-ME). Long-term X-band dual-polarization measurements and disdrometer DSD parameter data, acquired in Athens (Greece), have been used to quantitatively and qualitatively compare SCOP-ME retrievals of median volume diameter D0 and intercept parameter NW with two existing rain microphysical estimation algorithms, and the SCOP-ME retrievals of rain rate with three available radar rainfall estimation algorithms. Error statistics for rain rate estimation, in terms of relative mean and root mean square error and efficiency, show that the SCOP-ME has low relative error if compared to the other three methods, which systematically underestimate rainfall. The SCOP-ME rain microphysics algorithm also shows a lower relative error statistics when compared to the other two microphysical algorithms. However, measurement noise or other signal degradation effects can significantly affect the estimation of DSD intercept parameter from the three different algorithms used in this study. Rainfall rate estimates with SCOP-ME mostly depend on the median volume diameter, which is estimated quite more efficiently than the intercept parameter. Through comparisons based on the long-term dataset is relatively insensitive to path-integrated attenuation variability and rainfall rates, providing relatively accurate retrievals of the DSD parameters when compared to the other two algorithms.

Powered by Editorial Manager® and Preprint Manager® from Aries Systems Corporation

Response to Reviewers
Click here to download Response to Reviewers: Reply_reviwers.doc

Reply to the comments of reviewer 2

We would like to thank the reviewer for his/her constructive comments. A point-to-point response to the reviewer comments and description of the revisions, made to the manuscript, are described below. In Italic we provide the reviewer comment and in normal font our response.

General Comments

This paper relies heavily on 2 manuscripts (one under review) and one submitted. I had to read both manuscripts before I could evaluate the one submitted to JHM. It would not serve well the readers of JHM to not have access to the as yet unpublished manuscripts of (Kalogiros et al. IEEE Trans 2012) submitted April 2012, about same time as the JHM manuscript submission date...and Kalogiros et al. 2012 submitted Jan 2012. I leave it to the editor to decide disposition as the IEEE Trans paper (on which the JHM depends on heavily) might not be available to JHM readers in a timely manner.

The paper of Kalogiros et al. (2012a) has been accepted for publication in the *IEEE Trans. Geosci. Remote Sens*. and soon is going to be printed. As additional information to the reviewers we have uploaded it as well as the other cited paper by Kalogiros et al. (2012b), which, due to increased length after its first revision, was resubmitted from *IEEE Geosci. Remote Sens. Letters* to *IEEE Trans. Geosci. Remote Sens.*, where it is currently under review.

Overall, I found this manuscript difficult to "read"..I did not count but the number of tables and figure panels exceeds the actual number of written pages! Many of the figures need to be in color. It is a rather ambitious undertaking to use X-band radar to first do to attenuation-correction of Z_H and Z_{DR}, and then to retrieve DSD parameters (Do and Nw) and then compare with 2DVD. The results are likely to be useful as database is relatively large though the statistics seems to be dominated by stratiform rain type.

Indeed, it is ambitious but these are the processing steps that have to be made for X-band radar data. We also note in the paper that stratiform rain data are dominating in the current dataset, even though there are considerable convective data (~10% of the total data) and we expect to collect more convective rain data in future campaigns. Finally, in order to make the paper more readable, as suggested by the reviewer, we have reduced the number of figures and tables.

While I understand that the retrieval algorithms have low parameterization errors, it is not entirely clear that radar measurement errors would not dominate the comparison with 2DVD (even if bias errors have been "removed").... and so reducing the parameterization error is only reducing one component of the error as the authors know well, i.e., radar error = parameterization error + measurement error + attenuation-correction error + other? Plus when comparing against point measurements there is the ever-present "point-to-area" variance. I think the authors should mention this at the outset.

Measurement errors contribute mainly to the random part of the error has been made with a typical accuracy of 1 dBZ for Z_H and 0.2 dB for Z_{DR}, assuming that bias calibration is accomplished. The bias calibration of Z_H and Z_{DR} is made using long term disdrometer data as described in Kalogiros et al. (2012b). The calibration of Z_{DR} is also improved using a real-time method, which is based on average Z_H-Z_{DR} relations also described in that paper. We now mention this calibration method in the second paragraph of section 3.

In the paper of Kalogiros et al. (2012a) the effect of calibration biases and random noise on the microphysics and rain algorithms were examined using simulations. For the above typical values of errors, it was found that the proposed algorithms are accurate within 20%. We note that without bias and random errors the accuracy of the algorithms is better that 5%. These findings from that paper are now mentioned in the second paragraph of section 3.

The critical issue in the improvement of parameterization algorithms is the bias (systematic) error introduced by the parameterization. This bias error is added to the total error and the difference from volume to point measurements, as the reviewer points out. The minimization of the bias parameterization error is significant as it was shown in Kalogiros et al. (2012a) by comparing simulations with measurement noise to disdrometer data. This is also proved in the current paper using radar data (for example, Figs. 6 and 7). We now mention this information in the text at the end of section 3b.

My guess is that the retrieval of Do using Dz (by the way credit should be given to Jameson who first showed that Zdr was more closely related to Dz as opposed to D_0) is an improvement over the usual D_0-Zdr power law or polynomial fits and the Zdr measurement error can be reduced by averaging so that it is much less than the parameterization error. On the other hand, Z_H/Nw forms an awfully "tight" relationship to D_0 (independent of mu variations as shown by Testud et al.) so in this case the radar measurement error would dominate. For R the radar measurement error too would tend to dominate, and being a doubly stochastic process the "point-to-area" variance would be an equally important contributor.

The work of Jameson (1983) is actually referenced in Chapter 7 of the book of Bringi and Chandrasekar (2001), which is given as a reference in the paper of Kalogiros et al. (2012a) for the direct dependence of Z_{dr} on the reflectivity-factor weighted mean axis ratio of raindrops r_z and not simply D_z as the reviewer mentions, but depends also on the effective slope parameter of the raindrops axis ratio against diameter. Thus, from our relation Eq. (3b) in the current paper it can be seen that Z_{dr} is not a function of D_z alone, but the ratio Z_H/K_{DP} is also highly involved. The rain parameterization as shown in Kalogiros et al. (2012a) by comparing simulations with measurement noise to disdrometer data and in the current paper using radar data (for example Figs. 6 and 7) is also considerably improved using the new algorithm (in comparison with other algorithms). We agree with the reviewer that averaging can reduce the random measurement error, but the parameterization (bias) error does not. We now mention this in the paper at the end of section 2b.

In the paper of Kalogiros et al. (2012a) an alternative formula, equivalent to Eq. (3c), for N_w estimation was given (Eq. 16a in the uploaded paper). Strictly speaking, there is a slight dependence of Z_H/N_W ratio on the DSD shape parameter μ and a Mie-related multiplicative factor, which is a function of D_z. But the dependence of Z_H/N_W on D_0 does not mean that D_0 is simply a well-known function of radar measurements (with measurement errors) with no parameterization error because N_W is parameterized too and its parameterization error is quite significant.

Specific Comments

1. Introduction: Too many references! My philosophy is only to give as many references as needed and that too of relevance to the topic of the manuscript. Also, to not only list references for its own sake, but also to give some background or terse sentence as to what the references' main conclusions are in relation to the topic at hand.

We reduced the number of references and discussed more the remaining ones.

2. Section 2:

a. The Fisher distribution is not described in terms of standard deviation (like Gaussian).

Every distribution has a standard deviation (as well as all the statistical moments). The Fisher distribution (distribution of vector orientation) is not controlled directly by a standard deviation *std (*more accurately described as the *circular standard deviation*, which is the circle containing 66% of the data*)* but from a parameter κ related to the width of the distribution (Chapter 2, Bringi and Chandrasekar 2001). The parameter κ is approximately $(81/std)^2$ and, thus, it can be said that the Fisher distribution is controlled indirectly by the standard deviation. We added the word “circular” in front of “standard deviation”.

b. Eq. 1 uses the power law fit for fall speed vs. D, which is not a good fit at all to the Gunn-Kinzer data.

As it is mentioned by Kalogiros et al. (2012a), the factor $f_{R2}(D_0)$ in Eq. (1) accounts for the more accurate exponential law (Atlas et al. 1973; Bringi and Chandrasekar 2001) which was used in the simulations, instead of a power law, for the terminal velocity of raindrops against their diameter. We now mention it in the text following Eq. (2).

c. Eq 3b: Do tends to 0 when Zdr=0 dB (spherical drops) and R tends to 0 as well. We know this is not true for example in drizzle. So what are the thresholds used for Kdp and Zdr in the retrievals?

Theoretically, Z_{dr} and R are not exactly zero but they tend to zero in drizzle. In Kalogiros et al. (2012a) the ranges of rain parameters in the simulations are given. In these ranges of parameters the algorithms are applicable. The lower limit for D_0 was 0.5 mm, which corresponds to values as low as 0.1 dB for Z_{dr}, and 0.2 deg km^{-1} for K_{dp}.

*d. Eq (3d): This is from 2DVD data. Some caveat as to whether its physically-based or due to statistical correlations? The estimate of mu is really biased by the concentrations in the first few bins of any disdrometer. My own experience suggests that in light rainfall mu should tend to 0 while in heavy rain with equilibrium-like DSDs, Do tends to constant and mu=(lambda)*Do-3.67. Generally, equilibrium-like DSDs tend to have positive mu around 3.*

Eq. (3d) was inferred from long-term disdrometer data given in Kalogiros et al. (2012a). Similar variation of μ with D_0 has been observed (constrained Gamma distribution) by other researches (Zhang et al. 2001; Vivekanandan et al. 2004) as mentioned in Kalogiros et al. (2012a). The relation $\mu=\Lambda*Do-3.67$ is an exact identity that comes out of the definitions of μ, Λ and D_0 of the Gamma distribution. The shape parameter is affected by small diameter bins ($D<0.5D_m$) but also by the large diameter bins ($D>1.5D_m$) as shown in Figure 4 of Bringi et al. (2003). The method of estimation of μ has a significant impact

on the estimated value of μ. In our case, N_w and D_m were computed using the DSD moments method (Bringi et al. 2003), but the shape parameter was estimated by best fit (using minimum absolute error to exclude outliers) of the normalized Gamma distribution to the measured DSD. The small diameter bins are less than the large diameter bins and, thus, contribute less in the fit.

Section 3:

a. What is the point of stratiform-convective separation? As far as I can tell, the retrievals of R etc don't change or do they? Fig. 1 shows no overlap of stratiform data points and convective ones. Surely just based on statistics one would expect some slight overlap eg. maybe because of transition rain types? Appendix II is one sentence long. Why not add to main text? By the way, the first reference to use Nw vs. Do to separate stratiform vs. convective rain and to compare with Steiner et al is Thura et al. (2010, JTECH).

The stratiform-convective separation is made in order to show that the retrievals are applicable to both types of rain, which is basically the purpose of the development of polarimetric algorithms. The purpose of plotting them in different colors is to highlight the difference of the classified stratiform and convective data. In the Montopoli 2008a paper (Table II) the coefficients of the linear relation that separates the convective from the stratiform are given. The D_m-N_w classification is based on the statistical indicators of Table III of the same paper. Our figure showed only the 2DVD data around (including standard deviation) these average linear relations. For this reason the two classes do not overlap. In the revised figure we added all 2DVD data and indicated with dashed lines the standard deviation around the average classification lines.

b. Is "Eff" the Nash-Sutcliffe factor? If so give reference.

Eff = 1 – VAR(error)/VAR(reference). A reference was given.

Nash, J. E. and J. V. Sutcliffe (1970), River flow forecasting through conceptual models

part I — A discussion of principles, Journal of Hydrology, 10 (3), 282–290.

c. The SCOP reference is not available yet. Why not give a few sentences about the main results from that paper e.g., generally attenuation-correction for Zdr is biased low relative to 2DVD?

As we mentioned above in the reply to the first general comment, we uploaded this paper as additional information to the reviewers. We also added the following text describing the main results of that paper:

“ Path attenuation of radar signal is significant especially for high-frequency radars (like X band). For the correction of path attenuation in rain the SCOP algorithm is used. This algorithm is a self-consistent polarimetric algorithm, based on the parameterizations of the specific attenuation coefficients and backscattering phase shift in rain derived by Kalogiros et al. (2012a) and applied with an iterative scheme to separate radar rays (Kalogiros et al. 2012b). As it shown by Kalogiros et al. (2012a), the parameterizations of the specific attenuation coefficients and backscattering phase shift are quite robust and independent of the constraining function of DSD shape parameter μ against D_0 Eq. (4d). This independence is due to the use of D_z in the parameterizations. Application to radar data and comparison with disdrometer data and other polarimetric algorithms presented in literature (Testud et al. 2000; Gorgucci et al. 2006) showed that this algorithm performed similarly or better than the other attenuation correction algorithms. However, all algorithms presented a systematic underestimation at high values of differential attenuation probably due to the presence of hail in the path of the radar beam during those cases, which are not considered in these algorithms.”

d. Either Fig.3 should in color or better yet as a bar graph. There is no real basis for commenting "hail in addition to rain" along the path when the final Zdr measured is < -1 dB. They do a self-consistency test in SCOP, which should not "pass" if in fact hail were present. There is some inconsistency between Kalogiros et al (2012b) who found

corrected Zdr to be too low for convective cells yet Fig. 3 shows corrected Zdr to be overestimated by 15% even at large PIA.

We prefer to use gray scale in order to keep the publication cost low. We don't think that color would add significant information. We changed Fig. 3 to bar graph with gray scale.

The self-consistency in SCOP has to do with the consistency of the parameterizations. These parameterizations are valid for rain and as expected the algorithm fails (underestimation of signal attenuation) when mixed-phase hydrometeors exist on the radar ray. Theoretically, with a self-consistency test like proposed in Kalogiros et al. (2012b) it should be possible to detect probable hail area.. However, we have not yet developed such an extension of the algorithm, which requires verification with known hail events

The attenuation correction underestimation, reported by Kalogiros et al. (2012b), was not generally for large PIA values but when the measured Z_{dr} was below -1 dB. In the current paper we mention that this underestimation occurs in case of strong convective cells and observed Z_{dr} less than -1 dB. We modified this sentence to be clearer as "in the cases of strong convective cells with for large PIAs (> 6 dB) and observed Z_{DR} less than -1 dB, the SCOP correction method was found to systematically underestimate"

Section 3a.

a. Why bring in HSS when so far you have relied on rME, rRMSE and Eff? X-label for Fig. 4 says rainfall rate threshold yet the text refers to rain rates. Which is it? Fig. 4 if retained should be color or mark the different estimators next to the curves themselves. Fig.5 should definitely be drawn as a bar graph. The top panel Y-label should be rME and not rRMSE.

The thresholds are simply upper range values of rainfall rate.

As we mentioned before we prefer to use gray scale for publication cost low. Color is not really adding information in this case. We added symbols to the line to get clearer. We also turned Fig. 5 to bar graph with gray scale. We corrected the y-label of the top panel.

b. In second paragraph referring to Table 2: The sentence…" It is evident that the two algorithms with lowest rME..." should be clarified. I could not find rME of 19-21% anywhere in Table 2. Next sentence on SCOP-ME..."higher Eff (by 10-21%)…." not "Eff (20-21%)…." This occurs in several other Sections and authors to please clarify the "increase" relative to actual numbers.

The description of that Table is corrected in the revised text.

Section 3b:

a. Gorgucci et al (2006) should be (2008), check the latter author list for accuracy.

It was corrected. The name of V. N. Bringi was removed from the reference of Gorgucci et al (2008).

b. fig. 6: Surely a substantial part of the scatter must be due to "point-to-area" variance as opposed to measurement error alone? The legend should be "log Nw" and not "Nw". Regarding table 3, and Eff of -0.17 for log Nw is not very good by any standard even when compared with Park of Gorgucci.

We agree that part of the scatter is due to radar volume versus point (disdrometer) measurement scale mismatch and spatial separation. We added this detail in the first paragraph of section 3b.. The legend was corrected to $\log_{10}(N_w)$.

The efficiency is slightly negative for SCOP-ME, but it is worse for the other algorithms. This results shows that N_w estimate by all algorithms is significantly affected by noise or other factors that contribute to data scatter as mentioned above. Still, SCOP-ME is better than the other algorithms.

*c. I am really surprised by Fig. 7 especially the mode of 1.4 mm for Do and 2.5 for log Nw via SCOP-ME method. Even if the mode is dominated by stratiform rain, the Nw of 316 /mm/m**3 is way too low. Compared with Bringi et al (2003), in stratiform rain, on average for Do of 1.4 mm, the Nw should be around 2500 /mm/m**3...roughly an order of magnitude higher. The authors need to explain this.*

There was an error in the construction of these plots. The correct $\log_{10}(N_w)$ range of values is shown in Fig. 6 and agrees with Bringi et al. (2003) and other studies. The figure have been reviewed and corrected according to reviewer comments.

d. I don't see the point of Fig. 8...if retained suggest in color or as bar graph. If all 3 algorithms have Eff < 0 then that is a strong statement that should in abstract as well as in conclusions. But I don't understand how R in eq 1 which involves Nw can do better in terms of Eff as in Table 4 (Eff>0.76 for SCOP-ME)?

We think that Fig. is useful as it shows error statistics versus PIA, which is significant information for the total attenuation values where the algorithms can be applied accurately and to show if there is some trend (i.e., algorithm failure) with increasing total attenuation. We changed Fig. 8 to bar graph with gray scale.

Rainfall rate estimate is also based on the power of D_0. The efficiency for D_0 is a lot better than N_w. Thus, N_w is only correctly estimated on average by the retrieval algorithms (SCOP-ME performs better on this) and rainfall rate estimate variations are due mainly to D_0 variations. We added this information in discussion of Table 3 in section 3a, the Conclusions section and the abstract. In addition, in Table 3 statistics of accumulated rainfall values (and, thus, averaging and reduction of noise is included) is shown. In Table 4, the statistics of D_0 and N_w do not have such a noise reduction. In the old Tables 4 and 5 (statistics for separate case studies) also different data selection criteria were used (rainfall rate, D_0 or N_w, thresholds). In order to avoid confusion in the statistics we kept only the statistics for the whole dataset.

Section 4:

a. In fig. 9 both left and right panels (two different events) appear identical to me plus they should be in color.

The panels were in color and they were different. The spatial distribution of accumulated rainfall and the color scales are different in the two events. Probably the reviewer was confused by the terrain-blocked sectors, which are of course the same in both events. However, in order to reduce the number of figures we removed Fig. 9 as the PPI scans do not add much on the comparison of the algorithms with the disdrometer.

b. Fig 10a: stratiform rain is exhibiting quite a large time variation in R implying some embedded convection. The 2DVD derived Do and Nw, on average are more reasonable here (Do= 1.2 mm and Nw= 3000) relative to fig. 7 for SCOP-ME.

Rainfall rate is low (<5 mm h^{-1}) and the variations are of the same scale, and, thus, they cannot be characterized as convection. As we mentioned in the reply to comment c for section 3b N_w in Fig. 7 was in error which was corrected. Figure 10 is now Fig. 9 in the revised paper.

*c. In paragraph 4 related to convective rain: Tables 5 and 6 should be Tables 4 and 5 (ie. Table 6 missing). I would say from Table 5 that it appears quite hopeless to estimate Nw given the Eff of best case 0.28 to worst case -0.04 for SCOP-ME. This should be a strong result stated in abstract and conclusions. Why it does not impact R in eq. 1 is a mystery to me. I feel that the exponent of Do**(-4) in eq. 3c will propagate the error from eq. (3a) in a dominant way.... due to attenuation-correction error in Zdr. That is why I question the need to find the Nw estimator with least parameterization error when other errors dominate.*

We agree with the reviewer as we also noted in the reply to comment d for section 3b above. N_w is only estimated correctly on average from the algorithms with SCOP-ME doing better on this. This high scatter of N_w estimates has been observed in other studies too. If more rain events where available with wider range of values the correlation of estimated N_w with disdrometer measurements would be probably higher.

Overall, the authors should reduce the number of figures or use color and bar graphs to illustrate their main points. The R and Do estimates are relatively an improvement using SCOP-ME over the 2 other algorithms but for Nw it seems all 3 are quite bad in terms of Eff or some other factor is playing a role.

We agree with the reviewers and these are the main conclusions from these work. We tried to reduce and improve the figures.

Reply to the comments of reviewer 3

We would like to thank the reviewer for his/her constructive comments. A point-to-point response to the reviewer comments and description of the revisions, made to the manuscript, are described below. In Italic we provide the reviewer comment and in normal font our response.

The paper is a valuable contribution to the field and it should be published with minor revisions. The work would benefit from a more careful grammar and style revision.

We tried to correct the grammar and generally the text in the paper.

Comments

It is not clear from this paper if the SCOP-ME algorithm treats the problem of attenuation correction separately from the rain microphysics retrieval part.

A microphysics parameter (D_z) is actually used in the attenuation correction algorithm. The attenuation correction algorithm (Kalogiros et al. 2012b) is a self-consistent iterative method based on parameterizations of specific attenuation coefficients from Kalogiros et al. (2012a), which are quite robust and independent of the constraining function of DSD shape parameter μ against the median volume diameter D_0 *in* rain. This independence is due to the use of the reflectivity weighted drop diameter D_z in the parameterizations. We included now this detail in the text following Eq. (5). We also uploaded both papers (Kalogiros et al. 2012a has been accepted for publication and will be soon printed) as additional information to the reviewers.

Page 5 Line 14: 10db per radar profile? I think it would not hurt to mention again that you are referring to the total path attenuation?

The specification “total path attenuation” was added in that sentence.

P 6: Please connect this statement better to the context of the paper: "In past works Anagnostou et al. (2009 and 2010) evaluated a modified ZPHI algorithm (Testud et al. 2000) for attenuation and rainfall estimation with NW normalization, using limited observations from mobile X-band dual-polarization radar over complex terrain basins".

We have changed it to:

"Anagnostou et al. (2009 and 2010) evaluated a modified ZPHI algorithm (Testud et al. 2000) for attenuation and rainfall estimation with N_W normalization, using observations from mobile X-band dual-polarization radar over complex terrain basins"

P 7 L 15: Why Rayleigh limit only. Is the Mie scattering considered?

As explained in Kalogiros et al. (2012a) the Rayleigh limit is used as the basis to add the Mie scattering effects with a multiplicative function of reflectivity weighted diameter. We have corrected the sentence as follows:

"The polarimetric rain microphysics algorithm SCOP-ME for X-band radars was based on relations valid at the theoretical Rayleigh scattering limit corrected by a multiplicative rational polynomial function of reflectivity-weighted raindrop diameter (D_z) to approximate the Mie character of scattering at these electromagnetic frequencies."

P 8: The equation 2 should appear before the statement in line 3. Please change order.

We have reordered the equation in a properly manner.

P 8 L 7: repeats lines 1-3

This repetition (D_0 and N_w are estimated from…) is removed now.

P 9 L 3: "nominator" should be replaced with numerator

It has been corrected.

P 11 L17: "well to" does not seem right

It is changed from “compares well to with” to “agrees with”.

P 12 L 6: different – difference

It has been corrected.

P 13 L 14: "for" – from

It has been corrected.

P 13 L 22 & L 23: "here after" - hereafter

It has been corrected.

P 31: corr column is not explained

This column is the value of the correlation between the reflectivity Z_h values measured by the radar and the disdrometer for each event. We added this information in the legend of that table.

Suggestion: Use color in graph (the pattern can remain for gray-scale presentation).

We added symbols in the lines of Fig.4 and change Figs. 3, 5 and 8 to gray-scale bar graphs instead of color in order to keep the publication cost low.

Optimum Estimation of Rain Microphysical Parameters from X-Band
Click here to download Additional Material for Reviewer Reference: TGRS-2012-00011.pdf

Evaluation of a new Polarimetric Algorithm for Rain-Path Attenua

Click here to download Additional Material for Reviewer Reference: TGRS_Kalogiros_et_al_RadarAttenuation.pdf

Revised Manuscript (non-LaTeX)
Click here to download Manuscript (non-LaTeX): JHM_Anagnostou_revised.doc

Performance evaluation of a new dual-polarization microphysical algorithm based on long-term X-band radar and disdrometer observations

[1]MARIOS N. ANAGNOSTOU [(1,2)], JOHN KALOGIROS [(2)], FRANK S. MARZANO [(1,5)], EMMANOUIL N. ANAGNOSTOU [(3)], MARIO MONTOPOLI [(4,5)], AND ERRICO PICCIOTI [(5)]

[(1)] *Department of Information Engineering, Sapienza University of Rome, Rome, Italy*

[(2)] *Institute of Environmental Research and Sustainable Development, National Observatory of Athens, Athens, Greece*

[(3)] *Department of Civil and Environmental Engineering, University of Connecticut, Storrs, CT, USA*

[(4)] *Department of Geography, University of Cambridge, Cambridge, UK*

[(5)] *CETEMPS Centre of Excellence, University of L'Aquila, L'Aquila, Italy*

Under revision in AMS Journal of Hydrometeorology

October 2012

[1]*Corresponding author address:* Dr. Marios N Anagnostou, Department of Information Engineering, Sapienza University of Rome, Via Eudossiana 18, 00184 Rome, Italy. E-mail: marios.anagnostou@uniroma1.it or ma111@engr.uconn.edu

Abstract

Accurate estimation of precipitation at high spatial and temporal resolution of weather radars is an open problem in hydrometeorological applications. The use of dual-polarization gives the advantage of multiparameter measurements using orthogonal polarization states. These measurements carry significant information, useful for estimating rain-path signal attenuation, raindrop size distribution (DSD) and rainfall rate. This study evaluates a new Self-Consistent with Optimal Parameterization attenuation correction and rain Microphysics Estimation algorithm (named SCOP-ME). Long-term X-band dual-polarization measurements and disdrometer DSD parameter data, acquired in Athens (Greece), have been used to quantitatively and qualitatively compare SCOP-ME retrievals of median volume diameter D_0 and intercept parameter N_W with two existing rain microphysical estimation algorithms, and the SCOP-ME retrievals of rain rate with three available radar rainfall estimation algorithms. Error statistics for rain rate estimation, in terms of relative mean and root mean square error and efficiency, show that the SCOP-ME has low relative error if compared to the other three methods, which systematically underestimate rainfall. The SCOP-ME rain microphysics algorithm also shows a lower relative error statistics when compared to the other two microphysical algorithms. However, measurement noise or other signal degradation effects can significantly affect the estimation of DSD intercept parameter from the three different algorithms used in this study. Rainfall rate estimates with SCOP-ME mostly depend on the median volume diameter, which is estimated quite more efficiently than the intercept parameter. Through comparisons based on the long-term dataset is relatively insensitive to path-integrated attenuation variability and rainfall rates, providing relatively accurate retrievals of the DSD parameters when compared to the other two algorithms.

1. Introduction

Weather radar can provide spatio-temporal rainfall observations that can support hydro-meteorological modeling and flood forecasting. Rain rate retrievals can be estimated from the single polarization radar measurement, i.e., the radar reflectivity (Marshall and Palmer 1948; Battan 1973; Atlas and Ulbrich 1990; Joss and Waldvogel 1990) using the traditional standard reflectivity-rainfall (Z–R) relation on a physical basis of additional convective–stratiform rain classification information (Anagnostou and Krajewski 1999). A Z–R relation is obtained by regression analysis of gauge measurements and radar reflectivity or from drop size distributions (DSD) measured by aircraft and in situ disdrometers. However, the standard Z–R relation does not carry enough information to account for the climatological and orographic uniqueness of each location and temporal changes of the DSD. Thus, it cannot provide accurate rainfall rate (R in mm h^{-1}) estimates for different types of storms that are associated with varying microphysical processes.

On the other hand, rainfall rate estimators can be derived from modern polarimetric radar observations, which are related to the DSD in the radar volume (Bringi and Chandrasekar 2001). Dual-polarization (or polarimetric) weather radars have a significant advantage over single-polarization systems because they allow multi-parameter measurements using orthogonal polarization states. Polarimetric measurements, apart from the horizontal polarization reflectivity (Z_H in dBZ), usually include the differential reflectivity (Z_{DR} in dB), the differential phase shift (Φ_{DP} in deg) and the co-polar correlation coefficient (ρ_{HV} unitless).

Polarization diversity has a significant impact on correcting for rain-path signal attenuation in attenuating frequency (C- and X-band) radar measurements, making these systems applicable in heavy precipitation estimation (Testud et al. 2000). The typical range of X-band radar can be short (60 – 120 km) compared to the long-range operational weather radars (consisting primarily of S-band, like the WSR-88D network in USA, and C-band radars like most of the radar networks in Europe), but X-band radar can be low-power, mobile and constitute a cost effective system for filling up gaps in existing national radar networks. Examples include monitoring small-scale basins

in mountainous regions and urban areas (Anagnostou et al. 2010; Park et al. 2005) where, due to the high spatial-resolution associated to X-band radars, flood forecasting with distributed hydrologic modeling could be more effectively carried out due to high-resolution rainfall forcing (Ogden et al. 2000; Maki et al. 2008). A major drawback in X-band rainfall estimation is the rain-path signal attenuation effect, which can be larger than 10 dB for heavy rain events causing significant errors in rainfall estimation. The fundamental aspect that brought X-band back to the interest of hydrometeorologists for rainfall estimation is that the co-polarization differential phase shift (Φ_{DP}) measurement can be used as a constraint parameter for the effective estimation of specific copolar (A_H), differential (A_{DP}), and rain attenuation profiles (Testud et al. 2000; Matrosov et al. 2005; Park et al. 2005; Anagnostou et al. 2009; Marzano et al. 2010).

Based on data from different hydro-climatic regimes, numerous studies have confirmed that the estimation of rain microphysics can be significantly improved by the use of polarimetric radar parameters (Ryzhkov and Zrnic 1996; Anagnostou et al. 2004; 2007; Matrosov et al. 2005; Park et al. 2005; Kim et al. 2010). The method by Gorgucci et al. (2006), which was proposed for C-band, and a more robust algorithm, proposed for S, C and X-band (Gorgucci et al. 2008), can provide an estimate of the two DSD governing parameters, namely the raindrop median diameter D_0 (mm) and intercept parameter N_W ($mm^{-1}m^{-3}$) of the assumed normalized Gamma distribution, by utilizing power-related radar parameters (Z_H and Z_{DR}), the specific differential phase shift K_{DP} (deg km^{-1}) and the slope parameter β of drop shape (axis ratio r) against rain droplet diameter. Park et al. (2005) adapted a method similar to Gorgucci et al. (2001) at X-band frequencies. Many studies have also proposed the estimation of the DSD parameters as part of rain attenuation correction and/or rain estimation algorithms. The method developed by Testud et al. (2000) provides estimates of N_W for C and X-band frequencies using an attenuation-correction algorithm using the differential phase shift Φ_{DP} as an external constraint within the attenuation-estimation method, whereas Matrosov et al. (2005) estimated D_0 by relating it with the attenuation-corrected Z_{DR} for X-band. The methods aforementioned are either two- or three-parameter physical-based ad hoc or empirical algorithms.

There is also a nonparametric estimation of DSD from slant-profile dual-polarized Doppler spectra observations, presented by Moisseev et al. (2006). Vulpiani et al. (2009) and Anagnostou et al. (2008) have developed a nonparametric approach to estimate the three governing parameters of DSD from S or C-band and X-band dual-polarization radar parameters on the basis of a regularized artificial neural network (NN) or a Bayesian approach, respectively.

Recent studies by Anagnostou et al. (2009, 2010) and Kalogiros et al. (2012a) have led to the development and demonstration of a new algorithm for both polarimetric attenuation correction in rain and rain parameter estimation (i.e., rain rate and DSD). Anagnostou et al. (2009 and 2010) evaluated a modified ZPHI algorithm (Testud et al. 2000) for attenuation and rainfall estimation with N_W normalization, using observations from mobile X-band dual-polarization radar over complex terrain basins. Kalogiros et al. (2012a and 2012b) showed that the new "Self-Consistent with Optimal Parameterization" (SCOP) attenuation correction and rain "Microphysics Estimation" (hereafter called SCOP-ME) algorithm can provide improved estimates of rain rate and DSD parameters when compared with existing algorithms on the basis of simulated radar data derived from long-term observed raindrop spectra. The objective of this work is to statistically evaluate the performance of SCOP-ME algorithm using an extensive database of actual X-band dual-polarization observations coincident with *in situ* measurements from a 2D-video disdrometer, acquired in Athens (Greece) in a period of 4 years. The statistical performances of the SCOP-ME algorithm are also evaluated with different rainfall rate and DSD estimation algorithms taken from the literature. The statistical error evaluation of the SCOP-ME algorithm is performed for the horizontal-polarization Z_H and differential Z_{DR} reflectivity observed with the radar and corrected for attenuation in rain against the corresponding radar products calculated from the 2DVD observed DSD as a function of different path-integrated attenuation (PIA) values in four different categories.

The paper is organized as follows. In section 2 the SCOP-ME algorithm is briefly described. In sections 3 and 4 the results of the quantitative (statistics) and qualitative (test case) comparison of the estimations from the SCOP-ME algorithm and two different rain microphysical estimation (i.e.,

median volume diameter D_0 and intercept parameter N_W) algorithms, found in the literature, against the disdrometer observed DSD parameters and three different radar rainfall estimation algorithms also taken from the literature, are presented. Finally, the conclusion in section 5 summarizes the results of this work.

2. Rain microphysics retrieval algorithm

The polarimetric rain microphysics algorithm SCOP-ME for X-band radars was based on relations valid at the theoretical Rayleigh scattering limit corrected by a multiplicative rational polynomial function of reflectivity-weighted raindrop diameter (D_z) to approximate the Mie character of scattering at these electromagnetic frequencies. The reflectivity-weighted mean diameter is given by $D_z=E[D^7]/E[D^6]$ [1], where D is the raindrop equivolume diameter and E stands for the expectation value. The expectation value is estimated in practice as the DSD-weighted integral over the whole range of diameter values. The algorithm was developed from T-matrix scattering simulations (Kalogiros et al. 2012a) for a wide range of DSD parameters, a variable raindrops axis ratio around the relationship given by Beard and Chuang (1987), a Fisher distribution with a circular standard deviation of 7.5° for canting angle distribution, and air temperature varying from 5 (^{o}C) to 20 (^{o}C). The maximum parameterization error of SCOP-ME is less than 5%. The rain drop size distribution (DSD) model used in the simulations was the normalized Gamma distribution $n(D)$, as presented in many polarimetric radar rainfall studies (Testud et al. 2000; Bringi and Chandrasekar 2001; Illingworth and Blackman 2002):

$$n(D) = N_W f(\mu) \left(\frac{D}{D_0}\right)^{\mu} exp\left[-(\mu + 3.67)\frac{D}{D_0}\right] \quad (1)$$

where $n(D)$ with units $m^{-3}mm^{-1}$ is the volume density, D_0 (mm) is the median volume diameter, N_W ($mm^{-1}m^{-3}$) is the intercept parameter and the μ (no units) shape parameter. The SCOP-ME rainfall rate relation is given by the following equation (Kalogiros et al. 2012a):

$$R=0.8106F_R(\mu)N_W D_0^{4.67} f_{R_2}(D_0) \quad (2)$$

where the factor $f_{R2}(D_0)$ accounts for an exponential relationship more accurate than the usual power law (Atlas et al. 1973; Bringi and Chandrasekar 2001) and for the terminal velocity of raindrops against their diameter. The median volume diameter D_0, the intercept parameter N_W and the shape parameter μ of the DSD are estimated from the polarimetric radar measurements Z_H, Z_{DR} and K_{DP} using the following equations. The function F_R (μ) is given by:

$$F_R(\mu)=0.6\cdot 10^{-3}\pi\cdot 3.78\frac{6}{3.67^4}\frac{(3.67+\mu)^{\mu+4}}{\Gamma(\mu+4)}\frac{\Gamma(\mu+4.67)}{(\mu+3.67)(\mu+4.67)} \quad (3)$$

where Γ indicates the Gamma function. The DSD governing parameters (D_0 and N_W) are estimated from the following relationships:

$$D_0=D_Z f_{D_0}(D_Z) \quad (4a)$$

$$D_Z=D_{Z_1} f_{D_{Z_1}}(D_{Z_1}), D_{Z_1}=0.1802\left[\frac{Z_H}{K_{DP}}\xi_{DR}^{-0.2929}(1-\xi_{DR}^{-0.4922})\right]^{1/3} \quad (4b)$$

$$N_W=3610\left[\frac{K_{DP}}{(1-\xi_{DR}^{-0.8893})}\right]D_0^{-4} f_{N_{W_2}}(D_Z) \quad (4c)$$

$$\mu=165e^{-2.56D_0}-1 \quad (4d)$$

where D_Z is the reflectivity-weighted mean diameter (mm), ξ_{DR} is the differential reflectivity in linear units (ratio of reflectivity at horizontal and vertical polarization) and the horizontal reflectivity Z_H in these relations is also given in linear units (mm^6m^{-3}). The constrained of the shape

parameter μ in Eq. (3d) was obtained from long-term disdrometer data as described in Kalogiros et al. (2012a) with a method of best fit of the normalized Gamma distribution to the measured DSD. The shape parameter was not estimated with a moments method like in Vivekanandan et al. (2004), because this involves estimation of high order moments of the DSD (up to 5^{th} or 6^{th} order moment), which are characterized by large error due to the measurement errors in the high tail (high raindrop diameter values) of the DSD. The available disdrometer data supported the idea of a constrained Gamma DSD and agree with Zhang et al. (2001) and Vivekanandan et al. (2004) for D_0 values less than 2 mm. The functions $f_p(D_Z)$, where the subscript p indicates the corresponding parameter, are third-degree rational polynomial regression functions which were found to describe adequately the Mie character of scattering and to include most of the dependence on D_Z:

$$f_p(D_Z) = \frac{\sum_{n=0}^{3} a_n D_Z^n}{\sum_{n=0}^{3} b_n D_Z^n} \quad (5)$$

The coefficients of the polynomials in the numerator and denominator of $f_p(Dz)$ are given in Table 1 of Appendix I for the corresponding relations.

Before applying the microphysical retrieval algorithm (as well all the algorithms presented in this section and the following sections), reflectivities Z_H and Z_{DR} are corrected for the attenuation in rain. Path attenuation of radar signal is significant especially for high-frequency radars (like X band). For the correction of path attenuation in rain the SCOP algorithm is used. This algorithm is a self-consistent polarimetric algorithm, based on the parameterizations of the specific attenuation coefficients and backscattering phase shift in rain derived by Kalogiros et al. (2012a) and applied with an iterative scheme to separate radar rays (Kalogiros et al. 2012b). As it was shown by Kalogiros et al. (2012a), the parameterizations of the specific attenuation coefficients and backscattering phase shift are quite robust and independent of the constraining function of DSD shape parameter μ against D_0 Eq. (4d). This independence is due to the use of D_z in the parameterizations. Application to radar data and comparison with disdrometer data and other

polarimetric algorithms presented in literature (Testud et al. 2000; Gorgucci et al. 2006) showed that this algorithm performed similarly or better than the other attenuation correction algorithms. However, all algorithms presented a systematic underestimation at high values of differential attenuation probably due to the presence of hail in the path of the radar beam during those cases, which are not considered in these correction algorithms (Marzano et al. 2010).

In addition, various rainfall and rain microphysics algorithms available in literature are evaluated in this work against the new polarimetric algorithm SCOP-ME. The "standard" reflectivity-to-rainfall relationship is the most widely used method in radar-rainfall estimation (hereafter called *R*-Z_H) as it relates directly to the radar reflectivity measured by any conventional weather radar:

$$R_{Z_H} = \alpha_1 Z_H^{\beta_1} \quad (6)$$

The coefficients (i.e., α_1 and β_1) of this algorithm were determined from radar data collected during the years 2005-2006 in the area of Athens (Greece) by Kalogiros et al. (2006) and tested with various radar datasets by Anagnostou et al. (2009 and 2010).

The differential phase shift-rainfall relationship (hereafter called *R*-K_{DP}), for X-band radars is on average nearly linearly related to the rainfall rate:

$$R_{K_{DP}} = \alpha_2 K_{DP}^{\beta_2} \quad (7)$$

Various researchers have adopted formulations, which are special cases of the following power-law expression (hereafter named "combined" or *R*-$Z_H Z_{DR} K_{DP}$):

$$R_{Z_H Z_{DR} K_{DP}} = a Z_H^b Z_{DR}^c K_{DP}^d \quad (8)$$

All the above-mentioned coefficients α_1, α_2, β_1, β_2, a, b, c and d are given in Table 2 of Appendix I and are obtained by performing a multiple regression of Eqs. (6) – (8) using T-Matrix simulations as in Kalogiros et al. (2006), Montopoli et al. (2008) and Marzano et al. (2010).

3. Results

The performances of the SCOP-ME rain microphysics algorithm and other algorithms, described in section 2, are evaluated using measurements from the National Observatory of Athens (NOA) high-resolution dual-polarization Doppler X-band radar (XPOL) in the period 2008 to 2011 in the urban area of Athens, Greece. XPOL is one of the first mobile research-quality radars that have been extensively used since 2000 in different scientific field experiments in US, Greece and Italy (Anagnostou et al. 2004, 2006a, 2006b, 2009 and 2010). XPOL was deployed at the NOA's premises 500 meters above the sea level (A.S.L.). The radar conducted PPI scans at three different antenna elevations (0.5, 1.0 and 1.5 deg.) over an azimuth sector scan of 120 – 330 (deg.) with 150 meters range resolution for a total range of 60 (km). Antenna rotation rate was 6° s^{-1} and the total time for a volume scan was about 3 minutes. An optical 2D-video disdrometer (2DVD) was deployed within 35 km range at a coastal area southeast of the XPOL site (see Fig. 1), providing high-temporal (1 minute) resolution drop size distribution measurements. There were no terrain obstacles in the path from the radar to the disdrometer.

Twenty-one (21) rain events of coincident XPOL and disdrometer observations with significant rain in the path between the radar and the disdrometer were selected from the above database (see Table 1). The selection of the cases was based on the quality control of the radar and the 2DVD observations. To limit the effects of the sampling differences and the separation in altitude between the disdrometer and the radar volume, only rain events with correlation greater than 0.5 between the disdrometer-derived and radar-observed reflectivity were selected. Furthermore, only the lower radar elevations (below 1 deg.) were used in order to avoid possible melting layer effects during some stratiform rain events. The bias calibration of Z_H and Z_{DR} is made using long term disdrometer

data as described in Kalogiros et al. (2012b). Furthermore, the calibration of Z_{DR} is also improved using a real-time method, which is based on an average Z_H-Z_{DR} relation. The effect of calibration biases and random noise on the SCOP-ME microphysics and rain algorithms was examined using simulations (Kalogiros et al. 2012a). For the above typical values of errors it was found that the proposed algorithms are accurate within 20%. We note that without bias and random errors the accuracy of the algorithms is better that 5%, as mentioned in section 2. However, a point to mention is that the measurement errors contribute mainly to the random part of the error assuming that bias calibration has been made with a typical accuracy of ~1 dBZ for Z_H and ~0.2 dB for Z_{DR}.

A rain classification procedure, similar to that of Montopoli et al. (2008a), was adopted to separate the stratiform from convective rain types in the disdrometer time series. The classification procedure is based on the criterion that stratiform rain tends to be horizontally uniform and low in intensity as opposed to the convective regime, which generally shows high intensities at short time periods. Following the procedure discussed by Montopoli et al. (2008a), the DSD features were compared in term of the mass-weighted mean diameter $D_M = D_0 (\mu+4)/(\mu+3.67)$ for a normalized Gamma DSD as a function of $\log_{10}N_W$. Fig. 2 indicates a classification separation between the stratiform and convective rain types using a linear least square fit applied to the values of D_M and $\log_{10}N_W$ from the 2DVD DSD observations, which agrees with the relationship from Montopoli et al. (2008a). The linear least square fit applied to all the coincident 2DVD with the XPOL values of D_M and $\log_{10}N_W$, as $\log_{10}N_W = p_1 D_M + p_2$ for both the stratiform and convective rain types. The values of the p_1 and p_2 are taken from Montopoli et al. (2008a), as shown in Table 2. Note that according to Table 1, there are 6 convective type events of maximum rainfall rate > 30 (mm h^{-1}) out of the 21 selected cases.

The statistical metrics for the evaluation of the algorithms includes: (1) the relative mean error (*rME*), which is defined as the mean of the error (i.e., difference between reference values and radar estimates), normalized by the mean of the reference values; (2) the relative root mean square error (*rRMSE*), normalized by the storm average derived from the reference values; (3) the efficiency

score (*Eff*) , described by Nash and Sutcliffe (1970), defined as the difference between unity and the ratio of the error variance to reference variance. *Eff* is a statistical measure of the variability of the error normalized by the natural variability of the estimated parameter and is scaled from -∞ to 1. A value of 1 indicates that the estimate is perfect. An efficiency value equal to 0 or negative indicates that the estimation is, respectively, no better or even worse than using simply the mean value of the predicted parameter.

Statistical error analysis of Z_H and Z_{DR}, observed by XPOL and corrected for attenuation is performed for different values of path-integrated attenuation (PIA) equal to 0.5–2 dB, 2–4 dB, 4–6 dB and >6 dB. PIA was determined by calculating the difference of the measured reflectivity by XPOL to the reflectivity calculated from disdrometer measurements using the T-matrix algorithm (Mishchenko, 2000). The analysis was performed for the lowest two radar elevations (0.5 and 1.0 deg.) and for Z_H and Z_{DR} greater than 10 dBZ and 0.5 dB, respectively. Figure 3 shows that the attenuation-corrected Z_H measurements have low *rME* (almost 1%) and *rRMSE* (around 10 – 13%) for all PIA categories. The efficiency score is also high (> 0.8) for values of PIA even higher than 6 dB. The point to note is that the performance of the attenuation correction algorithm is nearly independent of the PIA. Evaluation for Z_{DR} shows slightly worse results at PIA values below 6 dB, which implies small intensity rainfall rates, exhibiting overestimation of about 15% and the relative RMSE in the range of 60% to 85%. However, as shown by Kalogiros et al. (2012b), in the cases of strong convective cells with for large PIAs (> 6 dB) and observed Z_{DR} less than -1 dB, the SCOP correction method was found to systematically underestimate, probably due to the presence of mixed-phase hydrometeors (hail in addition to rain) in the path of the radar beam.

a. Rainfall rate error statistics

The bulk statistics are performed as a function of the four different PIA ranges (i.e., 0.5 – 2 dB, 2 – 4 dB, 4 – 6 dB and >6 dB) and for values of reference rainfall rates greater than 0.1 mm h^{-1}. The rainfall error statistics are performed for the three above mentioned rainfall estimation algorithms (i.e., R-Z_H, R-K_{DP} and R-$Z_H Z_{DR} K_{DP}$) and SCOP-ME. For evaluation of the rainfall algorithms, in

addition to the *rME*, *rRMSE* and *Eff*, we also used the Heidke skill score (*HSS*), which measures the correspondence between the estimate and the reference (Barnston 1992; Conner and Petty 1998). The one–dimensional (1D) plot of *HSS* values at different rainfall rate thresholds is presented in Fig. 4. The SCOP-ME has a higher *HSS* compared to R-Z_H and R-K_{DP}, and similar to the R-$Z_HZ_{DR}K_{DP}$ algorithm at low rainfall rates (<4 mm h^{-1}), which contribute 94% of the cumulated rainfall. For medium to high rainfall rates (5 – 12 mm h^{-1}) SCOP-ME exhibits better performance compared to all other three retrieval methods.

Table 3 summarizes the bulk statistics of the algorithm estimates for different time integrations (15, 30 and 60) in rainfall (mm). It is evident from the table that the two algorithms with the lowest *rME* (range from 0.03 to 0.04 and -0.17 to -0.16), *rRMSE* (range from 0.51 to 0.63 and 0.60 to 0.69) and *Eff* (range from 0.79 to 0.83 and 0.73 to 0.87) are the SCOP-ME and R-$Z_HZ_{DR}K_{DP}$ algorithms, respectively. The quite good statistics of the SCOP-ME rainfall algorithm Eq. (2) despite the significant error of N_W (as shown in section 3b below is due to the dependence on the power of D_0. As shown in the section, the efficiency for the estimation of D_0 is significantly better than N_w. Thus, N_w is estimated correctly only on average from the algorithms (SCOP-ME performs better than the other algorithms examined in this work) and rainfall rate estimate variations are due mainly to D_0 variations. Overall, SCOP-ME outperforms all three algorithms in terms of the examined error statistics, having 3 to 12 times less *rME* and higher *Eff* (10 – 21%) scores.

Figure 5 presents the error metrics for the three different rainfall estimation algorithms and SCOP-ME versus PIA. Similarly to Fig. 3, the SCOP-ME algorithm has very low *rME* (ranging between 1% and 5% in absolute values) and it is nearly insensitive to PIA. It also has the largest *Eff* (0.82 to 0.73) and the smallest *rRMSE* (0.8 to 0.65) values. On the other hand, the R-Z_H rainfall algorithm suffers from large errors at high PIAs, while the combined method R-$Z_HZ_{DR}K_{DP}$ performs better when compared to the other two methods. A point to note is that the *rME* of the combined method exhibits a slight increase (~2% in absolute values) with respect to PIA. Dependency on PIA indicates that the combined algorithm is more sensitive to the attenuation correction errors.

b. Rain microphysics error statistics

This section investigates the accuracy of the estimation of DSD normalized Gamma model parameters from XPOL observations. The SCOP-ME algorithm error statistics are compared against two algorithms from the literature, the Park et al. (2005) (hereafter called Park) and the Gorgucci et al. (2008) (hereafter called Gorgucci). Error statistics were evaluated, as in previous sections, through comparison against the 2DVD DSD observations. Figure 6 shows scatter plots of the XPOL estimates of two DSD parameters (N_w and D_0) against parameters derived from 2DVD observations using the DSD moments method (Bringi et al. 2003). The x-axis indicates the reference disdrometer observations while the y-axis shows the radar estimates. The upper two panels are the radar estimates from SCOP-ME algorithm, the middle one is the "Gorgucci" estimates and the lower one is the "Park" estimates. The scatter plot shows similar variability in all algorithms, which is probably due to the measurement error effects and part of it is due to radar volume versus point (disdrometer) measurement-scale mismatch and spatial separation. However, the bulk statistics evaluated on the above data (see Table 4) shows a very low *rME* for the SCOP-ME algorithm (-0.03 and 0.04) and notably higher efficiency scores (0.37 and -0.17) for both D_0 and N_W estimates, when compared to the "Park" and "Gorgucci" algorithms. The efficiency is slightly negative for SCOP-ME but it is worse for the other algorithms. This results show that N_w estimate, by all algorithms, is significantly affected by noise or any other factors that contribute to data. Still, SCOP-ME is better than the other algorithms.

Figure 7 presents the joint frequency plots of the two DSD parameters ($\log_{10}N_W$ versus D_0). We note similarities in terms of size dimensions (on both the estimate and reference, the D_0 ranges between 1.1 and 1.8, and $\log_{10}N_W$ between 2 and 4) and the average slope of $\log_{10}Nw$-D_0 relation in the radar retrievals and the reference parameters. As shown in this figure, the core of the SCOP-ME density is more frequent than the reference, but it exhibits a lower error bias with respect to reference measurements. The "Gorgucci" estimates give a slope that is similar to the slope of the

reference measurements, but with significant bias. As shown in Fig. 6, this is due to combination of D_0 underestimation and $\log_{10}N_w$ overestimation in the "Gorgucci" estimates.

Figure 8 presents the bulk statistics of the error of the DSD parameters estimated from radar against the parameters derived from the 2DVD spectra observations (for Z_H values > 20 dBZ, D_0 > 0.5 mm and $\log_{10}N_W > 1$ mm^{-1}m^{-3}) versus PIA. The SCOP-ME estimates exhibit the lowest *rME* (-0.5% to 2% for D_0 and 1 to 3% for $\log_{10}N_W$) and are insensitive to PIA. Similarly, *rRMSE* ranges from 11.7% to 12.7% for D_0 and 11.5% to 12.5% for $\log_{10}N_W$ and week dependence on PIA. On the other hand, the other two methods exhibit moderate dependence on PIA especially in the case of to the $\log_{10}N_W$ estimates. Specifically, the *Eff* score of $\log_{10}N_W$ estimation is below zero, indicating weakness of the ability of these algorithms to capture the variability of the parameter. In the case of *rME*, a point to note is that both "Park" and "Gorgucci" methods systematically underestimate D_0 and overestimate $\log_{10}N_W$ (see Fig. 6). The *rRMSE* of D_0 estimates ranges from 16% – 17% for the "Gorgucci" and is around 14% for the "Park". A significant dependence of the "Gorgucci" D_0 estimate on PIA is noted. Similar results are observed in Table 4 for the $\log_{10}N_W$ estimates, since the SCOP-ME method has small *rME* (equal to 0.04) and *rRMSE* (equal to 0.14). The "Park" method shows results (0.09 for *rME* and 0.15 for *rRMSE*) similar to the SCOP-ME, whereas the "Gorgucci" method systematically tends to overestimate (*rME* equal 0.24) with the *rRMSE* close to 0.19. The SCOP-ME method also exhibits a better *Eff* (equal to -0.17) when compared to the other two methods, the "Gorgucci" and the "Park" methods having a large negative *Eff* values equal to -1.15 and -0.31, respectively.

In summary, the critical issue in the improvement of polarimetric microphysical algorithms is the systematic error (bias) introduced by the model parameterization. This bias error is added to the total error and the discrepancy due to volume-to-point measurement scale differences. Even though averaging could reduce the random measurement error, it cannot reduce the parameterization (bias) error. The minimization of the parameterization error is significant, as it was shown in Kalogiros et al. (2012a) by comparing simulations with measurement noise to disdrometer data. This is also

proved in the current paper using radar data (for example, Figs. 6 and 7) compared to the other algorithms.

4. Case study analysis

In this section the evaluation of the rain algorithms is performed qualitatively with a visual interpretation of case studies. The latter includes time series of selected rain events and total rain accumulation maps. The presented rain events are the 28/03/2008 event, which is a stratiform type rain event and the 14/01/2008 event, which is a short duration convective type event. These events are used to compare the spatial differences of the four radar rainfall algorithms and the two microphysical estimation algorithms and their temporal covariance with corresponding rain microphysics observations from the 2DVD data.

Figures 9a and 9b present time series (with 15 min temporal resolution) of radar rainfall rate (in mm h^{-1}) and DSD parameter (D_0 and $\log_{10}N_W$) estimates and disdrometer observations for the two rain events. The first case (stratiform event) evolves in two phases. The duration of the first phase is about 2 hours with its peak of about 5 mm h^{-1} at 8:00 UTC. The second phase of the event started in the afternoon (15:00 UTC) of the same date and dissipated just before midnight. In the second phase there are three rainfall peaks each one of about 3 mm h^{-1}. The figure shows that the SCOP-ME algorithm follows well the variations of the disdrometer observations if compared to the other algorithms.

In the convective rain event a short-duration rainfall rate peak of ~35 mm h^{-1} is observed at midday. During the peak rainfall the SCOP-ME and the combined algorithm are the two algorithms performs better. Tables 5 and 6 verify that those estimates are also in closer agreement with the disdrometer observations. The SCOP-ME and the combined methods are the two algorithms with the best bulk statistics (0.13 and 0.07 for *rME*, 0.34, 0.22 for *rRMSE* and 0.98 and 0.99 for *Eff*) for the rainfall rate estimate. Regarding the DSD parameter estimation, the SCOP-ME shows a performance comparable with the "Gorgucci" method in terms of *rME* for the D_0 parameter estimation (0.05 and -0.02, respectively), whereas for the $\log_{10}N_W$ parameter retrieval SCOPE-ME

shows the best performance. Furthermore, SCOP-ME shows better performances in terms of *rRMSE* (15% and 23%) and *Eff* scores (0.60 and -0.04) for D_0 and $\log_{10}N_W$ DSD parameter estimates, respectively.

5. Conclusions

The performance of a new combined "Self-Consistent with Optimal Parameterization" attenuation correction and rain "Microphysics Estimation" (SCOP-ME) algorithm for polarimetric X-band radars was investigated in this study. The proposed method performance was compared against three other radar rainfall algorithms (R-Z_H, R-K_{DP} and R-$Z_HZ_{DR}K_{DP}$) and two DSD retrieval algorithms ("Parks" and Gorgucci"), derived from the literature. The evaluation included data collected during a three-year period (2008 to 2011) with an X-band dual-polarization Doppler weather radar and coincident DSD observations from a 2D-video disdrometer (35 km range from the radar) in the urban area of Athens, Greece.

The SCOP-ME polarimetric rainfall and microphysics algorithm was developed from T-matrix simulations at X-band, based on the Rayleigh scattering limit relations with the addition of a rational polynomial dependence on reflectivity weighted droplet diameter D_Z due to Mie scattering effects. The algorithm is based on the consideration that Gamma distribution model can adequately describe the shape of raindrop size distribution. For the evaluation of the SCOP-ME algorithm a statistical error analysis of the horizontal-polarization Z_H and differential Z_{DR} reflectivity observed with the radar and corrected for attenuation in rain against the corresponding radar products calculated from the 2DVD observed DSD was performed as a function of different path-integrated attenuation values in four different categories (0.5 – 2, 2 – 4, 4 – 6 and >6 dB). The corrected for rain attenuation Z_H and Z_{DR} overall showed very good performance with low relative error compared to the measured ones. We have showed that the correction of Z_H is nearly independent of PIA.

Error statistics of the three rainfall estimation algorithms and the SCOP-ME algorithm, evaluated against the disdrometer rainfall observations, showed that the SCOP-ME has a low relative error in

all PIAs categories compared to the other three methods, while the other algorithms systematically underestimate rainfall. The efficiency statistics, determined from SCOP-ME estimates, exhibited better results at low to moderate (0.5 – 4 dB) PIAs and comparable results at large (>4 dB) PIAs to the "combined" R-$Z_H Z_{DR} K_{DP}$ rainfall algorithm. The Heidke skill score statistic had comparable results of the SCOP-ME with the R-$Z_H Z_{DR} K_{DP}$ rainfall algorithm at low rainfall rates (<4 mm h^{-1}), while for moderate to high rainfall rates (4 – 12 mm h^{-1}) SCOP-ME exhibited better results.

The SCOP-ME rain microphysics algorithm was also compared to two existing DSD parameter estimation algorithms. Overall, SCOP-ME was shown to have a lower relative error statistics when compared to the other algorithms. The SCOP-ME algorithm performed better for all PIA ranges and rainfall rates and provided relatively accurate retrievals of the DSD parameters. However, the estimation of N_w by all algorithms is significantly affected by noise or other factors like radar volume versus point (disdrometer) measurement scale mismatch and spatial separation. Thus, N_w is estimated correctly only on average from all algorithms. The good statistics for rainfall rate estimate with SCOP-ME are due mainly to D_0 variation, which is usually estimated quite more effectively than N_w.

Although the study included a long-term dataset, the latter is still to be considered limited in terms of hydro-climatic regime variability. Additional studies, based on data from different climatic regions (i.e., tropical, oceanic, and complex terrain, etc.) and more extensive ground validation observations are needed to verify the extended performance and also the generalization capability of SCOP-ME retrieval technique for different storm types and radar ranges. Furthermore, future work should focus on precipitation classification (snow, hail, graupel in addition to rain) and development of radar microphysics algorithms for each precipitation type. Neural networks and fuzzy logic are tools to be considered in future extensions of this work.

Acknowledgments. This work is part of the HYDRORAD project (Research for SMEs category – Grand Agreement number FP7-SME-2008-1-232156) funded by EC 7th Framework Program from 2009 until 2011. Marios N. Anagnostou thanks the support of the Marie Curie Fellowship under the Grant Agreement Number 236871 HYDREX, coordinated by the Sapienza University of Rome, Italy and the support of the Postdoctoral Fellowship by the Greek General Secretariat for Research and Technology under the Grant Agreement Number PE10(975) HYDRO-X, coordinated by the National Observatory of Athens, Greece, in the framework of the program "Education and Lifelong Learning" funded by Greece and EU-European Social Fund.

APPENDIX I

The values of the coefficients of the rational polynomial functions of Eq. (5) in the parameterization of rainfall rate by Eqs. (2) - (4) at X-band (9.37 GHz) are reported in Table A1 and fitted coefficients of Eqs (6 – 8) from the simulated spectra DSD in Table A2. It is worth noting that the simulated radar observables for the regression analysis, used to estimate the coefficients of Eqs. (7 – 8) in Montopoli et al. 2008b, are DSD spectra taken from seven different climatological regions (i.e., three from Japan, two from US, one from UK and one from Greece). Moreover, in the simulated radar observables three different types of noise due to instrumental, reconstruction and attenuation correction errors are included.

References

Anagnostou, E. N., and W. F. Krajewski, 1999: "Real-time radar rainfall estimation. Part I: Algorithm formulation." *J. Atmos. Oceanic Technol.*, Vol. 16, pp. 189 – 197.

Anagnostou, E. N., Anagnostou, M. N., Krajewski, W. F., Kruger, A., and B. J. Miriovsky, 2004: "High-resolution rainfall estimation from X-band polarimetric radar measurements." *J. Hydrometeor.*, Vol. 5, pp. 110 – 128.

Anagnostou, E. N., Grecu, M., and M. N. Anagnostou, 2006a: "X-band polarimetric radar rainfall measurements in Keys area Microphysics project." *J. Atmos. Sci.*, Vol. 63, pp. 187 – 203.

Anagnostou, M. N., Anagnostou, E. N., and J. Vivekananda, 2006b: "Correction for Rain-Path Specific and Differential Attenuation of X-band Dual-Polarization Observations." *IEEE Trans. Geosci. Rem. Sens.*, Vol. 44, pp. 2470 – 2480.

Anagnostou, M. N., Anagnostou, E. N., and J. Vivekanandan, 2007: "Comparison of Raindrop Size Distribution Estimates from X-Band and S-Band Polarimetric Observations." *IEEE Geosci. Rem. Sens. Let.*, Vol. 4, pp. 601 – 605.

Anagnostou, M. N., E. N. Anagnostou, G. Vulpiani, M. Montopoli, F. S. Marzano, and J. Vivekanandan, 2008: "Evaluation of X-band polarimetric radar estimates of drop size distributions from coincident S-band polari- metric estimates and measured raindrop spectra," *IEEE Trans. Geosci. Remote Sens.*, Vol. 46, pp. 3067 – 3075.

Anagnostou, M. N., J. Kalogiros, E. N. Anagnostou, and A. Papadopoulos, 2009: "Experimental results on rainfall estimation in complex terrain with a mobile X-band polarimetric weather radar." *Atmos. Res.*, Vol. 94, pp. 579 – 595.

Anagnostou, M. N., J. Kalogiros, E. N. Anagnostou, M. Tarolli, A. Papadopoulos, and M. Borga, 2010: "Performance evaluation of high-resolution rainfall estimation by X-band dual-polarization radar for flash flood applications in mountainous basins." *J. Hydrol.*, Vol. 394, pp. 4 – 16.

Atlas, D., and C. W. Ulbrich, 1990: "Early foundations of the measurement of rainfall by radar." Radar in Meteorology. *American Meteorological Society, Boston, USA*, pp. 86–97.

Barnston, A. G., 1992: "Correspondence among the correlation, RMSE, and Heidke forecast verification measures; refinement of the Heidke score." *Wea. Forecasting*, Vol. 7, pp. 699 – 709.

Battan, L.J. (1973): "Radar observations of the atmosphere," University of Chicago Press, Chicago, 323 p.

Beard, K.V., and C. Chuang, 1987: "A new model for the equilibrium shape of raindrops." *J. Atmos. Sci.*, Vol. 44, pp. 1509 – 1524.

Borowska, L., A. Ryzhkov, D. Zrnić, C. Simmer, and R. Palmer, 2011: "Attenuation and differential attenuation of 5-cm-wavelength radiation in melting hail." *J. Appl. Meteor. Climatol.*, Vol. 50, pp. 59 – 76.

Brandes, E. A., Zhang, G., Vivekanandan, J., 2004: "Drop size distribution retrieval with polarimetric radar: Model and Application." *J Appl. Meteor.*, Vol. 43, pp. 461 – 475.

Bringi, V. N., and V. Chandrasekar, 2001. Polarimetric Doppler Weather Radar. Cambridge University Press, Cambridge, UK. 662pp.

Bringi, V. N., V. Chandrasekar, J. Hubbert, E. Gorgucci, W. L. Randeu, and M. Schoenhuber, 2003: "Raindrop size distribution in different climatic regimes from disdrometer and dual-polarized radar analysis." J. Atmos. Sci., Vol. 60, pp. 354 – 365.

Bringi, V. N., Tang, T., and V. Chandrasekar, 2004: "Evaluation of a new polarimetrically based Z–R relation." *J. Atmos. Ocean. Technol.*, Vol. 21, pp. 612 – 623.

Cifelli, R., V. Chandrasekar, S. Lim, P. C. Kennedy, Y. Wang, and S. A. Rutledge, 2011: "A new dual-polarization radar rainfall algorithm: application in Colorado precipitation events." *J. Atmos. Oceanic Technol.*, Vol. 28, pp. 352 – 364.

Gorgucci, E., Scarchilli, G., Chandrasekar, V., and V. N. Bringi, 2001: "Rainfall Estimation from Polarimetric Radar Measurements: Composite Algorithms Immune to Variability in Raindrop Shape–Size Relation." *J. Atmos. Ocean. Tech.*, Vol. 18, pp. 1773 – 1786.

Gorgucci, E., V. Chandrasekar, and L. Baldini, 2006: "Correction of X-band radar observation for propagation effects based on the self-consistency principle." *J. Atmos. Ocean. Technol.,* Vol. 23, pp. 1668 – 1681.

Gorgucci, E., V. Chandrasekar, and L. Baldini, 2008: "Microphysical retrievals from dual-polarization radar measurements at X band." *J. Atmos. Oceanic Technol.,* Vol. 25, pp. 729 – 741.

Conner, M. D., and G. W. Petty, 1998: "Validation and intercomparison of SSM/I rain-rate retrieval methods over the continental Unites States." *J. Appl. Meteor.,* Vol. 37, pp. 679 – 700.

Gourley, J. J., P. Tabary, and J. P. DuChatelet, 2007: "algorithm for the separation of precipitating from non-precipitating echoes using polarimetric radar observations." *J. Atmos. Oceanic Technol.,* Vol. 24, pp. 1439 – 1459.

Heinselman, P. L., and A. V. Ryzhkov, 2006: "Validation of polarimetric hail detection," *Weather Forecast.,* Vol. 21, pp. 839 – 850.

Hubbert, J. V., and V. N. Bringi, 1995: "An iterative filtering technique for the analysis of coplanar differential phase and dual-frequency radar measurements." *J. Atmos. Oceanic Technol.,* Vol. 12, pp. 643 – 648.

Illingworth, A. J., and T. M. Blackman, 2002: "The need to represent raindrop size spectra as normalized gamma distributions for the interpretation of polarization radar observations." *J. Appl. Meteor.,* Vol. 41, pp. 286 – 297.

Ishimari, A., 1991. Electromagnetic Wave Propagation, Radiation, and Scattering. Prentice Hall. 637pp.

Joss, J., and A. Waldvogel, 1990: "Precipitation measurements and hydrology." In: Atlas, D. (Ed.), Radar in Meteor. Amer. Meteor. Soc, Boston, pp. 577–606.

Kalogiros, J, M. N. Anagnostou, E. N. Anagnostou, 2006: "Rainfall retrieval from polarimetric X-band radar measurements." *Proceedings of 4th European Conference on Radar in Meteorology and Hydrology (ERAD),* Barcelona, Spain, pp. 145–148.

Kalogiros, J., M. N. Anagnostou, E. N. Anagnostou, M. Montopoli, E. Picciotti, and F. S. Marzano, 2012a: "Optimum estimation of rain microphysical parameters using X-band dual-polarization radar measurements," submitted to the *IEEE Trans. Geosci. Remote Sens.*

Kalogiros, J., M. N. Anagnostou, E. N. Anagnostou, M. Montopoli, E. Picciotti, and F. S. Marzano, 2012b: "Evaluation of an iterative polarimetric algorithm at X-band for path attenuation correction in rain against disdrometer data," to be submitted to the *IEEE Geosci. Remote Sens. Letters*.

Kim, D.-S., M. Maki, and D.-I. Lee, 2010: "Retrieval of three-dimensional raindrop size distribution using X-band polarimetric radar." *J. Atmos. Oceanic Technol.*, Vol. 27, pp. 1265 – 1285.

Liu, H., and V. Chandrasekar, 2000: "Classification of hydrometeors based on polarimetric radar measurements: development of fuzzy logic and neuro-fuzzy systems, and in situ verification." *J. Atmos. Oceanic Technol.*, Vol. 17, pp. 140 – 164.

Maki, M., and Coauthors, 2008: "X-band polarimetric radar network in the Tokyo metropolitan area—X-NET." *Proceedings of 5th European Conf. on Radar in Meteorology and Hydrology (ERAD), Helsinki, Finland*, S3.7.

Marzano, F. S., G. Botta and M. Montopoli, 2010: "Iterative Bayesian Retrieval of Hydrometeor Content from X-band Polarimetric Weather Radar." *IEEE Trans. Geosci. Rem. Sens.*, Vol. 48, pp. 3059 – 3074.

Marshall, J.S and W. McK. Palmer (1948): "The distribution of raindrops with size." *J. Meteor.*, Vol. 5, pp. 165 – 166.

Marzano F.S., G. Botta and M. Montopoli, 2010, "Iterative Bayesian Retrieval of Hydrometeor Content from X-band Polarimetric Weather Radar", IEEE Trans. Geosci. Rem. Sensing, ISSN: 0196-2892, Vol. 48, pp. 3059-3074.

Matrosov, S. Y., D. E. Kingsmill, B. E. Martner, and F. M. Ralph, 2005: "The Utility of X-Band Polarimetric Radar for Quantitative Estimates of Rainfall Parameters." *J. Hydrometeor.,* Vol. 6, pp. 248 – 262.

Matrosov, S. Y., K. A. Clark, and D. E. Kingsmill, 2007. "A Polarimetric Radar Approach to Identify Rain. Melting-Layer, and Snow Regions for Applying Corrections to Vertical Profiles of Reflectivity". *J. Appl. Meteor. Climatol.,* Vol. 46, pp. 154 – 166.

Mishchenko, M. I., 2000: "Calculation of the amplitude matrix for a nonspherical particle in a fixed orientation." *Appl. Opt.,* Vol. 39, pp. 1026 – 1031.

Moisseev, D. N., V. Chandrasekar, C. M. H. Unal, and H. W. J. Russchenberg, 2006: "Dual-polarization spectral analysis for retrieval of effective raindrop shapes," *J. Atmos. Ocean. Technol.,* Vol. 23, pp. 1682 – 1695.

Montopoli, M., G. Vulpiani, M. N. Anagnostou, E. N. Anagnostou, and F. S. Marzano, 2008a: "Processing disdrometer raindrop spectra time series from various climatological regions using estimation and autoregressive methods," *IEEE Trans. Geosci. Remote Sens.,* Vol. 46, pp. 2778 – 2787.

Montopoli, M., F. S. Marzano, and G. Vulpiani, 2008b: "Analysis and synthesis of raindrop size distribution time series from disdrometer data," *IEEE Trans. Geosci. Remote Sens.,* Vol. 46, pp. 466 – 478.

Nash, J. E. and J. V. Sutcliffe (1970), River flow forecasting through conceptual models part I — A discussion of principles, Journal of Hydrology, 10 (3), 282–290.

Ogden, F. L., H. O. Sharif, S. U. S. Senarath, J. A. Smith, M. L. Baeck, and J. R. Richardson, 2000: "Hydrologic Analysis of the Fort Collins, Colorado, Flash Flood of 1997", *J. Hydrology,* Vol. 228, pp. 82 – 100.

Park, S.-G., M. Maki, K. Iwanami, V. N. Bringi, V. Chandrasekar, 2005a: "Correction of Radar Reflectivity and Differential Reflectivity for Rain Attenuation at X Band. Part I: Theoretical and Empirical Basis". J. Atmos. Ocean. Tech., Vol. 22, pp. 1621 – 1632.

Pruppacher, H. R., and K. V. Beard, 1970: “A wind tunnel investigation of the internal circulation and shape of water drops falling at terminal velocity in air.” *Quart. J. Roy. Meteor. Soc.*, Vol. 96, pp. 247 – 256.

Rico-Ramirez M. A., and I. D. Cluckie, 2008: “Classification of ground clutter and anomalous propagation using dual-polarization weather radar.” *IEEE Trans. Geosci. Rem. Sens.*, Vol. 46, pp. 1892 – 1904.

Ryzhkov, A. V., and D. Zrnic´, 1996: “Assessment of rainfall measurement that uses specific differential phase.” *J. Appl. Meteor.*, Vol. 35, pp. 2080 – 2090.

Testud, J., E. Le Bouar, E. Obligis, M. Ali-Mehenni, 2000: “The rain profiling algorithm applied to polarimetric weather radar.” *J. Atmos. Ocean. Technol.*, Vol. 17, pp. 332 – 356. Vivekanandan, J. G. Zhang, and E. Brandes, 2004: “Polarimetric radar estimators based on a constrained gamma drop size distribution model.” *J. Appl. Meteorol.*, Vol. 43, pp. 217-230.

Vulpiani, G., S. Giangrande, and F. S. Marzano, 2009: “Rainfall estimation from polarimetric S-band radar measurements: validation of a neural network approach.” *J. Appl. Meteor. Climatol.*, Vol. 48, pp. 2022 – 2036.

Zhang, G., J. Vivekanandan, and E. Brandes, 2001: “A method for estimating rain rate and drop size distribution from polarimetric radar measurements.” *IEEE Trans. Geosci. Remote Sens.*, Vol. 39, pp. 830 – 841.

LIST OF TABLES

LIST OF FIGURES

FIG. 1. Experimental area showing the radar site (NOA) and the in situ 2D-video disdrometer site (GV1). On the right, we show the pictures of the XPOL at NOA, and the disdrometer at the GV1 site.

FIG. 2. Scatter plot of the mean diameter (D_m) against the intercept parameter $\log_{10}$ (N_W). The two least square fits (taken from the Montopoli et al. 2010) of the data points are shown for the stratiform (C – light grey bold line and circle data points) and convective (S – black bold line and circle data points) cluster.

FIG. 3. Bulk error statistics (*rME*, *rRMSE* and *Eff*) of radar observed and corrected for specific attenuation horizontal polarization reflectivity (left panels) and Differential reflectivity (right panels) versus the Path Integrated Attenuation (PIA).

FIG 4. One-dimensional HSS plot versus rainfall rate (mm h^{-1}) threshold.

FIG. 5. Bulk error statistics (*rME*, *rRMSE* and *Eff*) of the four radar rainfall algorithms versus PIA.

FIG. 6. Scatter plots of radar estimated (SCOP-ME, "Park" and "Gorgucci") D_0 and $\log_{10}N_W$ versus calculated from 2DVD observed spectra.

FIG. 7. 2D-frequency contour plots of $\log_{10}N_W$ (N_W in $mm^{-1}m^{-3}$) versus D_0 (in mm).

FIG. 8. Bulk statistics (*rME*, *rRMSE* and *Eff*) of radar estimated $\log_{10}N_W$ (N_W in $mm^{-1}m^{-3}$) and D_0 (in mm) parameters versus PIA (dB).

FIG. 9a. Timeseries of the 28/03/2008 rain event for a) rainfall rates from the four radar rainfall algorithms and the 2DVD rainfall rate observations and b) DSD parameters from the three different microphysical algorithms and the parameters calculated from the 2DVD measured spectra.

FIG. 9b. Similar to Fig. 9a, but for 01/14/2008 rain event.

TABLES

TABLE 1. Selected rain cases with corresponding statistical analysis for each event. The first column is the date of the event. The "corr" column shows the value of the correlation between the reflectivity Z_H values measured by XPOL and the 2DVD for each event. The columns labelled "max", "mean", "%rain > 1 mm h^{-1}" and "%rain > 10 mm h^{-1}" stand for the statistics of 2DVD (the left hand side of each column) and XPOL (the right hand side of each column).

dt/mon/yr	**corr**	**max (**mm h^{-1})		**mean (**mm h^{-1})		**%rain > 1 mm**		**%rain > 10 mm h^{-1}**	
14/01/08	0.88	81.4	130.3	11.7	12.7	31.8	34.9	10.6	10.6
28/03/08	0.79	13.0	9.6	1.3	1.9	46.8	60.7	0.7	0.0
02/04/08	0.8	34.0	33.8	5.7	4.6	87.2	83.5	14.9	8.8
05/04/08	0.88	17.9	14.8	2.0	2.0	41.2	43.2	2.0	1.5
22/09/08	0.63	2.5	2.1	1.3	1.3	73.3	66.7	0.0	0.0
25/09/08	0.84	87.8	53.6	29.5	20.6	64.0	80.0	48.0	48.1
17/11/08	0.68	11.7	8.7	2.4	2.0	35.2	34.6	0.6	0.0
29/11/08	0.78	13.0	15.7	3.5	2.7	75.0	67.5	5.0	2.5
02/01/09	0.78	4.7	7.9	0.8	0.9	17.6	24.2	0.0	0.0
05/01/09	0.78	4.1	5.3	1.0	1.1	38.3	41.3	0.0	0.0
08/01/09	0.64	14.3	9.4	3.8	2.7	31.0	31.0	3.5	0.0
13/01/09	0.69	4.5	6.8	1.3	1.6	39.0	40.4	0.0	0.0
31/01/09	0.51	5.1	37.5	1.8	6.5	66.7	88.1	0.0	15.1
08/02/09	0.76	12.5	9.4	3.7	2.7	62.5	57.1	3.6	0.0
05/03/09	0.81	11.0	10.3	2.8	2.5	84.6	83.5	1.2	1.1
12/03/09	0.69	4.0	6.1	1.2	1.7	47.7	58.1	0.0	0.0
21/03/09	0.63	16.0	37.5	4.0	5.7	75.5	77.4	4.7	1.4
05/04/09	0.59	0.6	1.5	0.3	0.7	0.0	2.9	0.0	0.0
17/10/09	0.76	2.1	2.0	0.7	0.9	16.9	27.7	0.0	0.0
25/10/09	0.75	31.5	25.7	2.4	2.4	61.6	75.3	3.4	4.1
12/11/10	0.82	29.5	53.2	4.2	8.7	12.5	17.6	4.2	8.0
16/01/11	0.48	6.1	8.5	2.1	2.9	76.0	86.0	0.0	0.0
27/01/11	0.59	7.8	7.8	2.1	2.2	70.6	66.7	0.0	0.0
02/02/11	0.57	3.0	11.1	0.7	2.6	09.4	24.3	0.0	0.7
18/02/11	0.54	3.8	7.5	1.0	1.5	14.9	16.6	0.0	0.0
20/02/11	0.52	14.7	16.8	1.1	1.8	16.9	29.2	1.5	3.1
02/03/11	0.78	5.3	5.3	1.3	1.3	54.8	59.6	0.0	0.0
29/03/11	0.56	3.9	3.9	1.0	1.5	34.1	59.7	0.0	0.0

TABLE 2. Coefficient for the D_M, $\log_{10}N_W$ linear relationship.

Cluster type	p_1	p_2
Stratiform	-2.51	6.68
Convective	-0.88	5.51

TABLE 3. Total bulk statistics in terms of rainfall (in mm) for the 4 different radar rainfall estimation algorithms compared with 2DVD DSD observations as a function of time integrations (15, 30 and 60 min).

15/30/60	**relative ME**	**relative RMSE**	**Efficiency**
SCOP-ME	0.04/0.03/0.04	0.63/0.59/0.51	0.82/0.79/0.83
R-Z_H	-0.21/-0.21/-0.18	0.81/0.77/0.74	0.70/0.65/0.64
R-K_{DP}	-0.37/-0.37/-0.37	0.72/0.73/0.69	0.76/0.69/0.69
R-$Z_H Z_{DR} K_{DP}$	-0.16/-0.17/-0.16	0.69/0.68/0.60	0.78/0.73/0.76

TABLE 4. Bulk statistics of the selected rain events for the three different radar rain microphysics estimation algorithms compared with 2DVD observations.

Park/Gorgucci/SCOP-ME	**relative ME**	**relative RMSE**	**Efficiency**
D_0 *(mm)*	-0.12/-0.16/-0.03	0.16/0.19/0.14	0.13/-0.31/0.37
$log_{10}N_W$ *(N_W in $mm^{-1}m^{-3}$)*	0.09/0.24/0.04	0.15/0.19/0.14	-0.31/-1.15/-0.17

TABLE A1. The values of the coefficients of the rational polynomial functions Eq. (5) in the parameterization of rainfall rate by Eqs. (2)-(4) at X-band (9.37 GHz).

Function	a_0/b_0	a_1/b_1	a_2/b_2	a_3/b_3
f_{D_0} in Eq. (4a)	0.9542/ 1.0000	0.2989/ 0.2243	0.0577/ 0.2949	0.0030/-0.005
$f_{D_{z1}}$ in Eq. (4b)	0.9190/ 1.0000	0.1501/-0.2248	-0.1722/ 0.0182	0.0511/ 0.023
$f_{N_{w2}}$ in Eq. (4c)	1.0000/ 1.0000	-0.6792/-0.6410	0.2112/ 0.1551	-0.0109/-0.006
f_{R2} in Eq. (4d)	1.0000/ 1.0000	-1.2313/-0.2176	2.1166/ 0.3064	0.6842/ 1.230

TABLE A2. Fitted coefficients of Eqs (6 – 8) from the simulated spectra DSD.

α_1	β_1	α_2	β_2	a	B	C	d
3.36×10^{-2}	0.58	11.37	0.98	1.88	0.25	-1.07	0.61

Figure 1
Click here to download Rendered Figure: FIGURE 1.docx

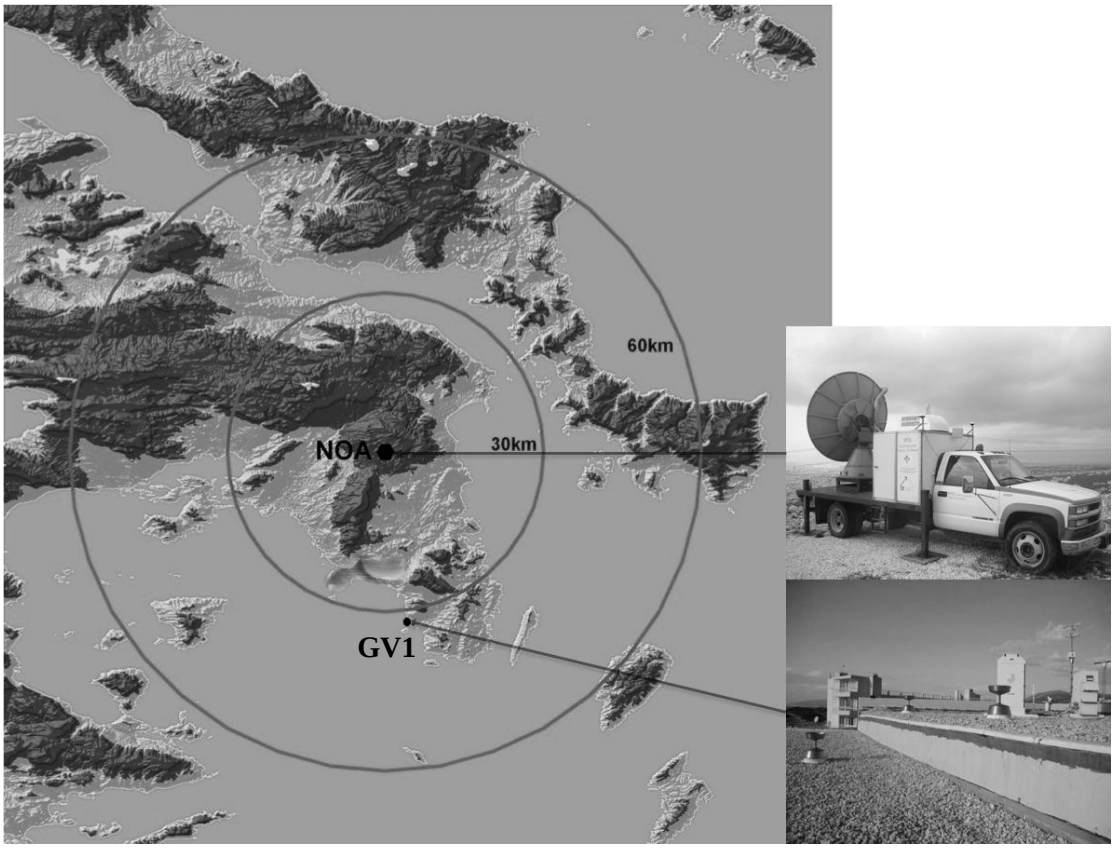

FIGURE 1. Experimental area showing the radar site (NOA) and the in situ 2D-video disdrometer site (GV1). On the right, we show the pictures of the XPOL at NOA, and the disdrometer at the GV1 site.

Figure 2
Click here to download Rendered Figure: FIGURE 2_1.docx

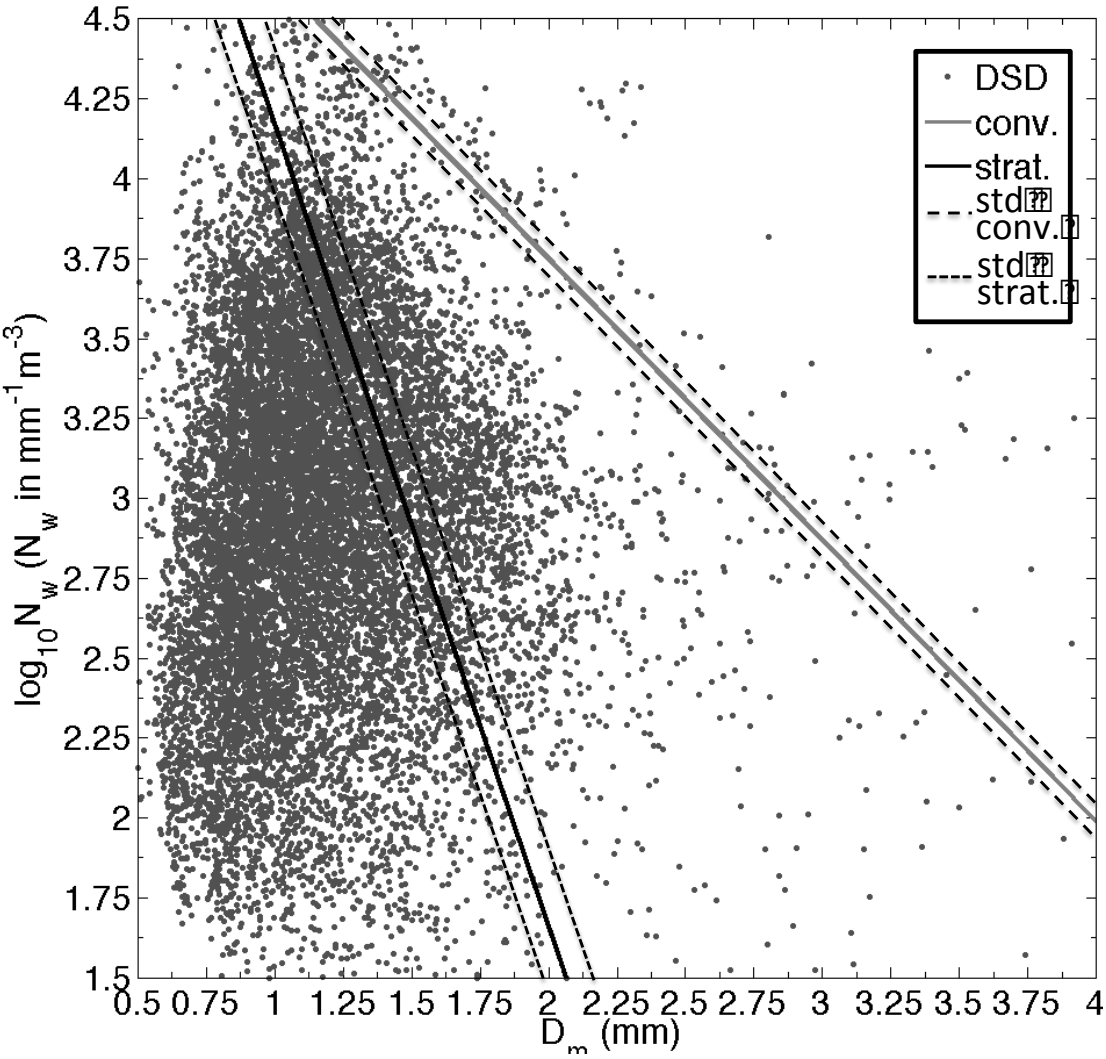

FIGURE 2. Scatter plot of the mean diameter (D_m) against the intercept parameter $\log_{10}$ (N_W). The two least square fits (taken from the Montopoli et al. 2010) of the data points are shown on the 2DVD's DSD observations.

Figure 3
Click here to download Rendered Figure: FIGURE 3_1.docx

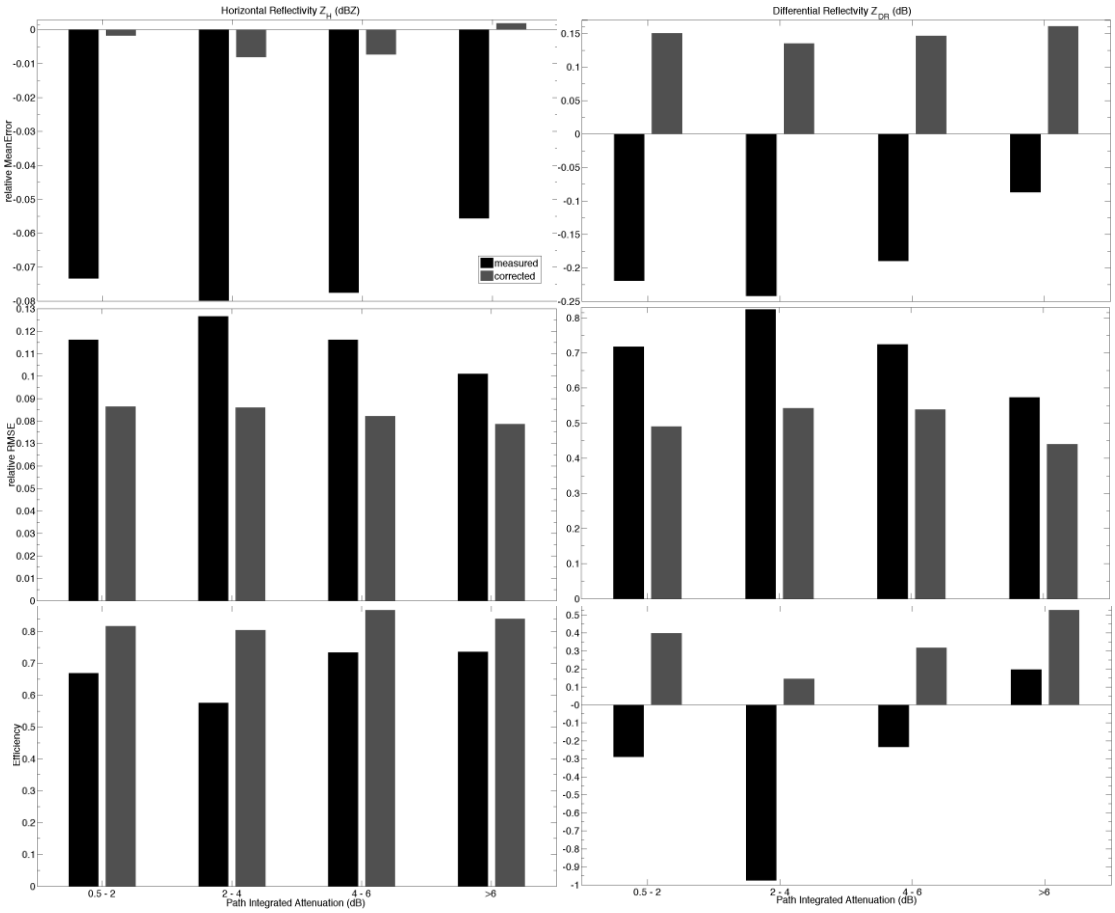

FIGURE 3. Bulk error statistics (*rME*, *rRMSE* and *Eff*) of radar observed and corrected for specific attenuation horizontal polarization reflectivity (left panels) and Differential reflectivity (right panels) versus the Path Integrated Attenuation (PIA).

Figure 4
Click here to download Rendered Figure: FIGURE 4_1.docx

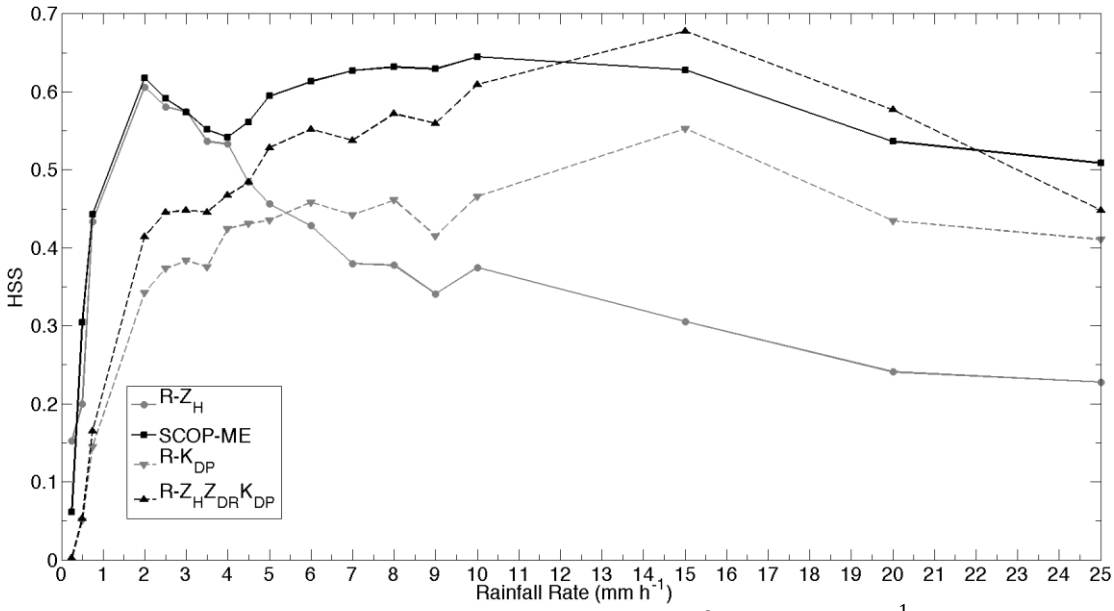

FIGURE 4. One-dimensional HSS plot versus rainfall rate (mm h^{-1}) threshold.

Figure 5
Click here to download Rendered Figure: FIGURE 5_1.docx

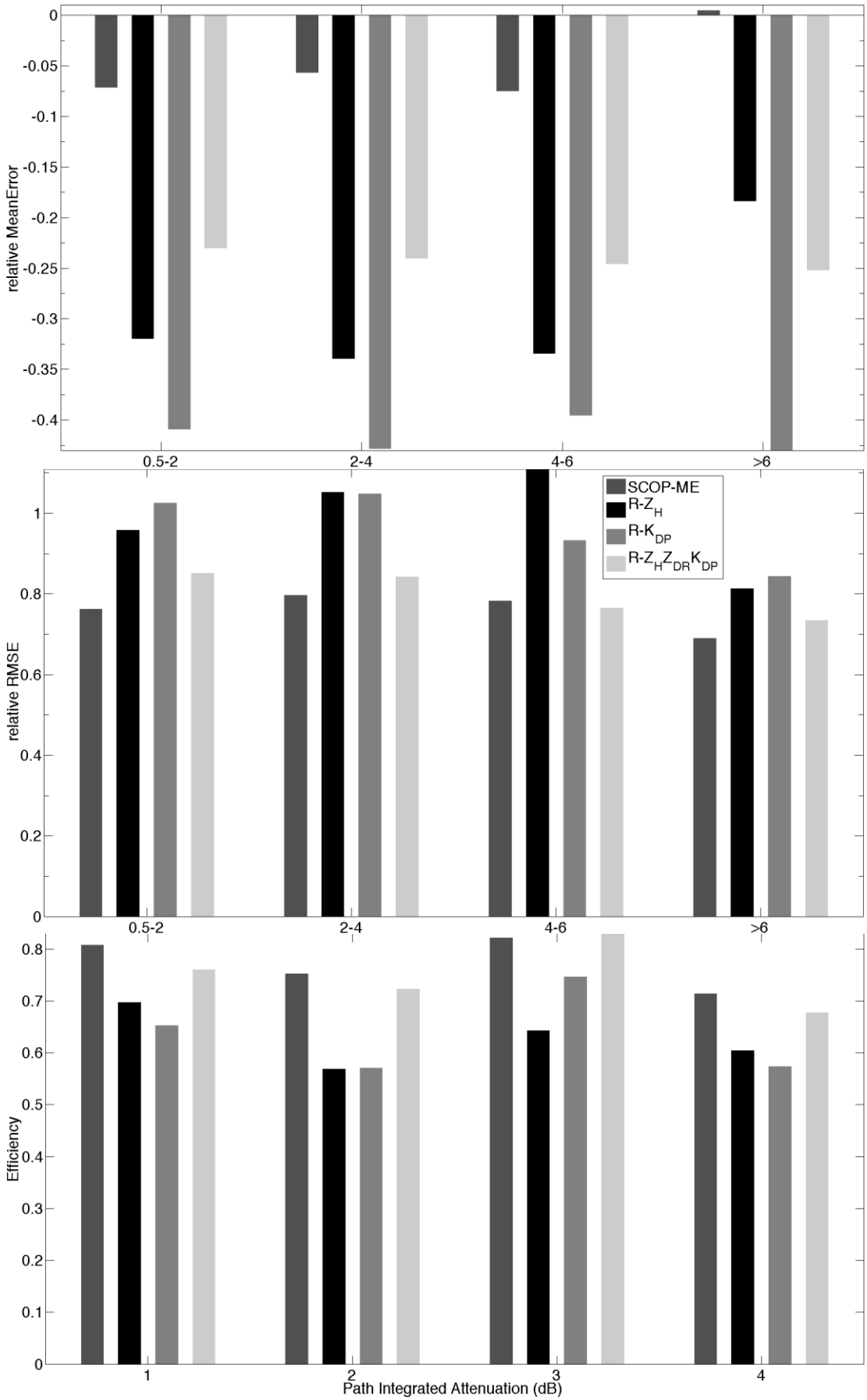

FIGURE 5. Bulk error statistics (*rME*, *rRMSE* and *Eff*) of the four radar rainfall algorithms versus PIA.

Figure 6
Click here to download Rendered Figure: FIGURE 6_1.docx

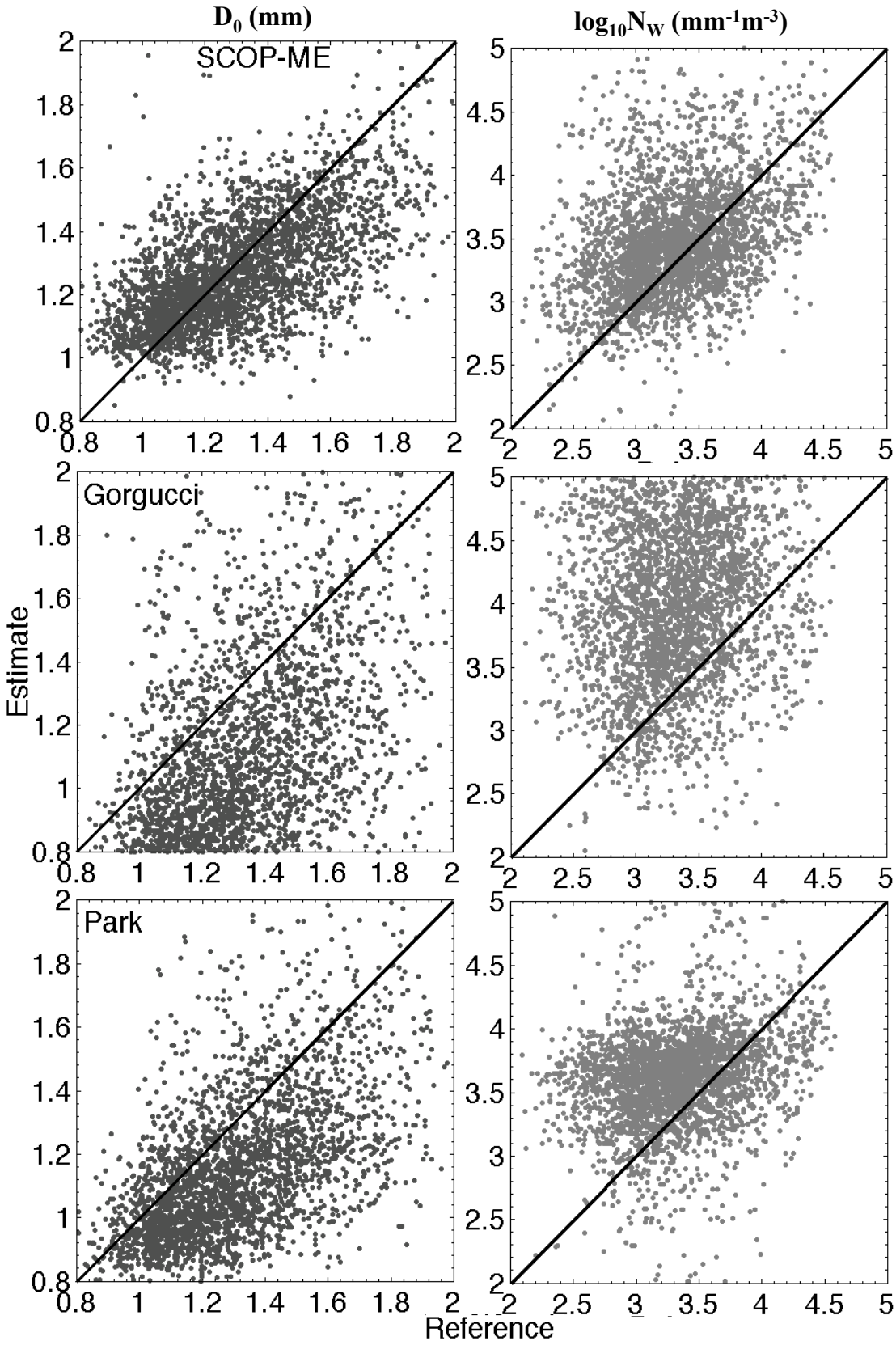

FIGURE 6. Scatter plots of radar estimated (SCOP-ME, "Park" and "Gorgucci") D_0 and $\log_{10}N_W$ versus calculated from 2DVD observed spectra.

Figure 7
Click here to download Rendered Figure: FIGURE 7_1.docx

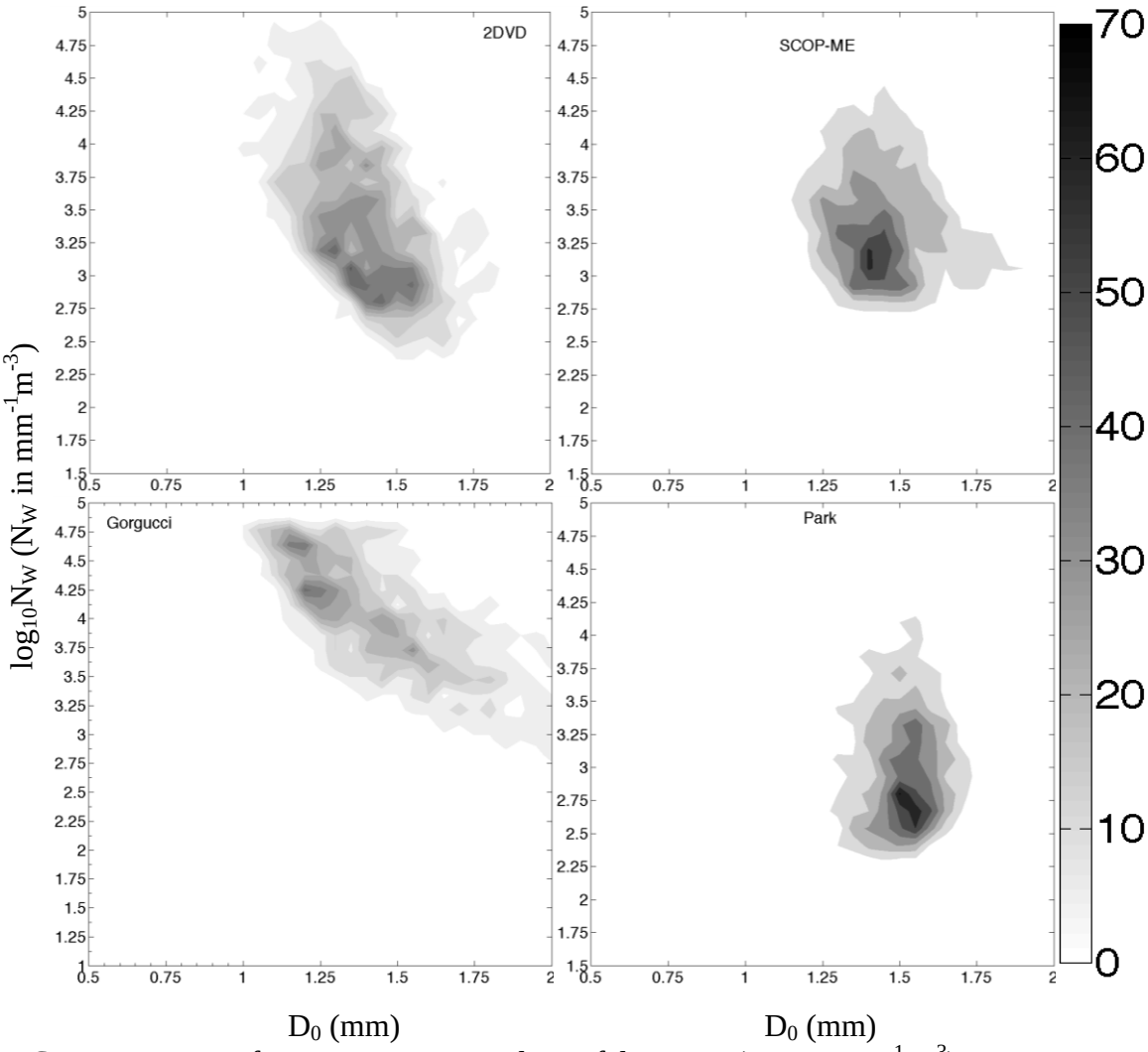

FIGURE 7. 2D-frequency contour plots of $\log_{10}N_W$ (N_W in $mm^{-1}m^{-3}$) versus D_0 (mm).

Figure 8
Click here to download Rendered Figure: FIGURE 8_1.docx

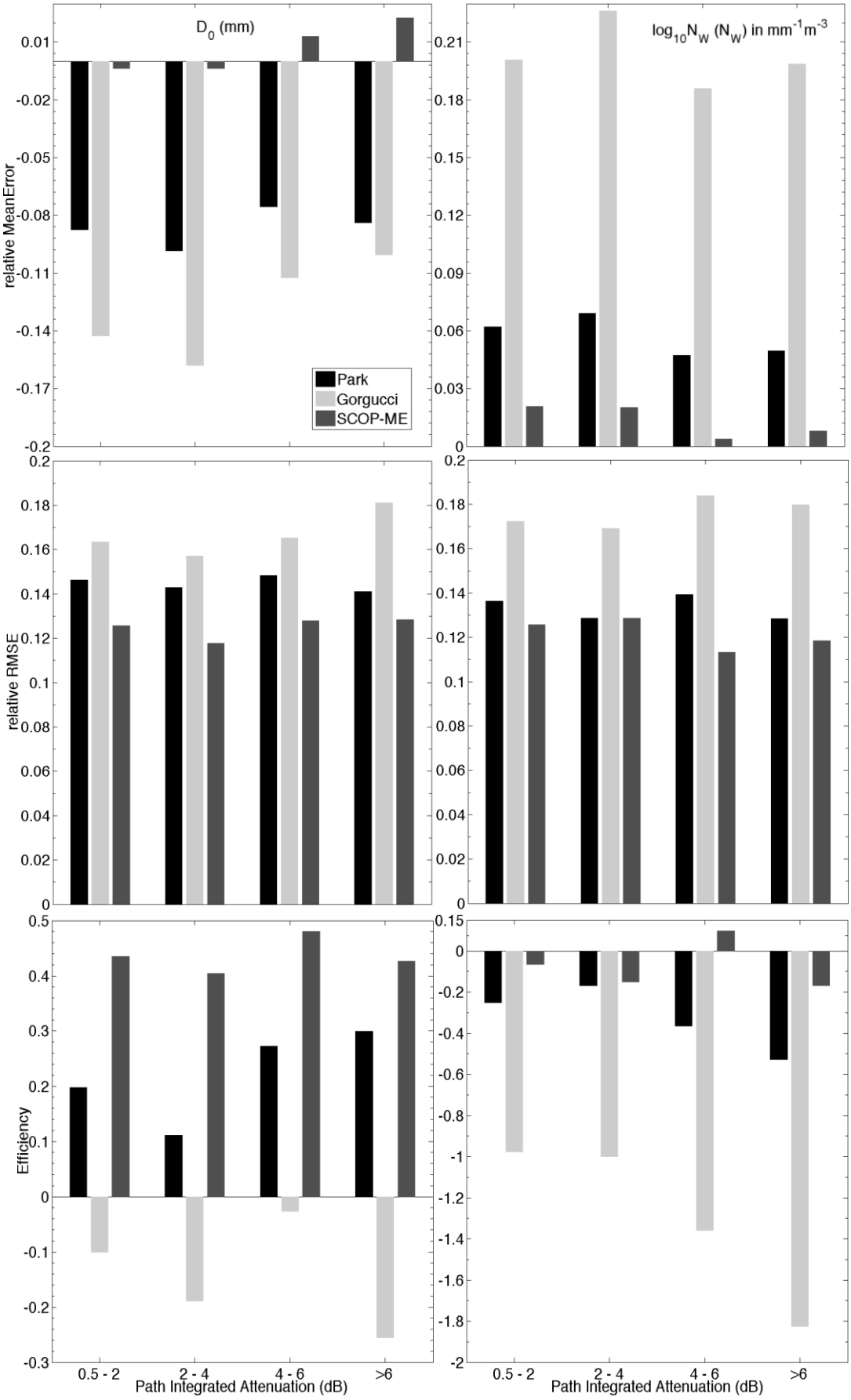

FIGURE 8. Bulk statistics (*rME*, *rRMSE* and *Eff*) of radar estimated $\log_{10}N_W$ (N_W in $mm^{-1}m^{-3}$) and D_0 (mm) parameters versus PIA (dB).

Figure 9a
Click here to download Rendered Figure: FIGURE 9a.docx

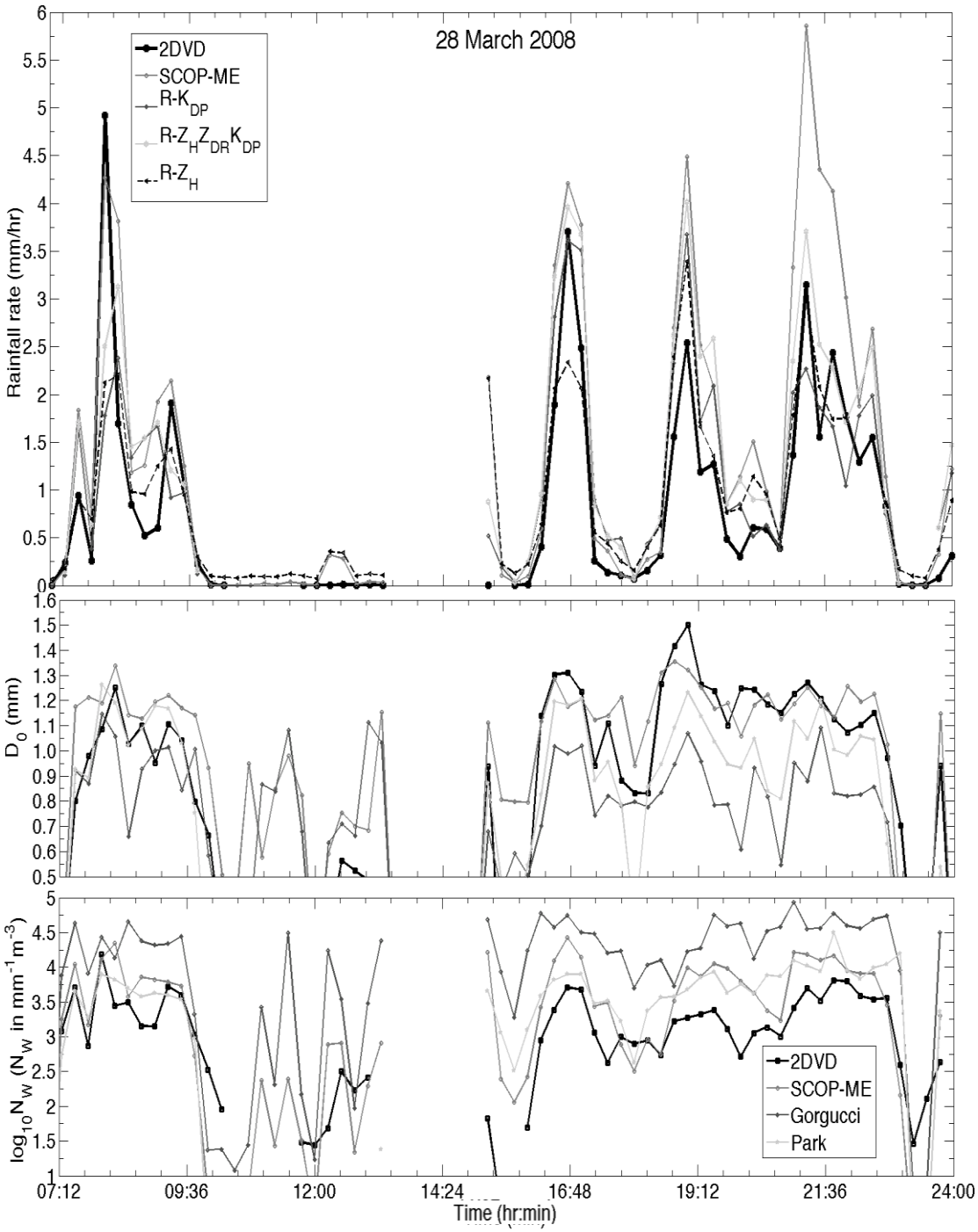

FIGURE 9a. Timeseries of the 28/03/2008 rain event for a) rainfall rates from the four radar rainfall algorithms and the 2DVD rainfall rate observations and b) DSD parameters from the three different microphysical algorithms and the parameters calculated from the 2DVD measured spectra.

Figure 9b
Click here to download Rendered Figure: FIGURE 9b.docx

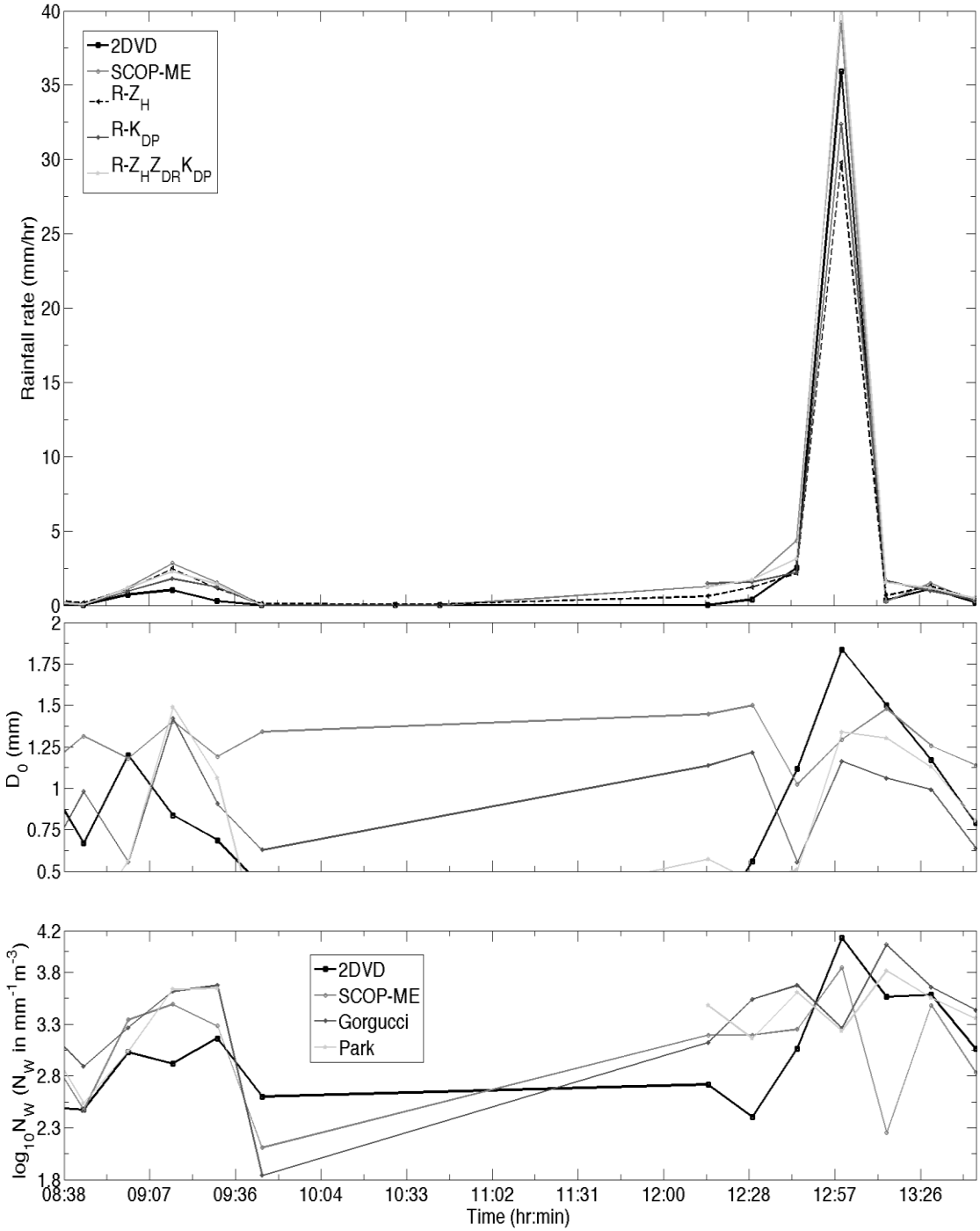

FIGURE 9b. Similar to Fig. 10a, but for 01/14/2008 rain event.